

Design and Modeling of Straight-Blade Vertical Axis Wind Turbine

A Final Year Project Report

Presented to

SCHOOL OF MECHANICAL & MANUFACTURING ENGINEERING

Department of Mechanical Engineering

NUST

ISLAMABAD, PAKISTAN

In Partial Fulfillment

of the Requirements for the Degree of

Bachelors of Mechanical Engineering

by

Muhammad Ahmad Saleem

Muhammad Ahsan Ali

Muhammad Hamza Naeem

Muhammad Huzefa

Graduation: June, 2021

EXAMINATION COMMITTEE

We hereby recommend that the final year project report prepared under our supervision by:

Muhammad Ahmad Saleem	00000208988
Muhammad Ahsan Ali	00000213389
Muhammad Huzefa	00000214567
Muhammad Hamza Naeem	00000208450

Titled: “Design and Modelling of Straight Blade VAWT” be accepted in partial fulfillment of the requirements for the award of DEGREE NAME degree with grade ____

Supervisor: Dr. Sadaqat Ali, Assistant Professor Dept. of Mechanical Engineering	<hr/> Dated:
Committee Member: Dr. M. Safdar, Asst. Professor Dept. of Mechanical Engineering	<hr/> Dated:
Committee Member: Dr. Rehan Zahid, Asst. Professor Dept. of Mechanical Engineering	<hr/> Dated:

(Head of Department)

(Date)

COUNTERSIGNED

Dated: _____

(Dean / Principal)

ABSTRACT

Pakistan is one of those countries which has large potential of energy harvest from renewable energy sources and specially from wind. With the surge of global warming, the world is moving towards cleaner and viable sources of energy. Horizontal Axis Wind Turbines (HAWT) currently dominates the most of the wind power farm markets in the world but Vertical Axis Wind Turbines (VAWT) are also capable of harvesting large amounts of energy with benefits over the HAWTS. VAWTS do not need a control system to be pointed in the direction of wind because with its blade in radial arrangement, wind from any direction is useful. In this report, a Straight-Blade VAWT is designed for low speeds and its performance parameters are also identified for which the improvement of the VAWT will be obtained. Self-starting ability of VAWT is also analyzed and stress and vibration analysis will be investigated in ANSYS Fluent

ACKNOWLEDGMENTS

First of all, we would like to thank ALLAH Almighty for giving us a chance and helping us bringing this project to a completion. Second, we extend our heartfelt gratitude to our supervisor, Dr. Sadaqat Ali, whose knowledge and thoughtful guidance enabled us in this project. We would like to thank our subject professors in SMME whose teachings built our concepts used in this project. At the end, we would like to thank our families for their unconditional support and prayers that helped us go throughout our Final Year Project duration.

ORIGINALITY REPORT

VAWT

ORIGINALITY REPORT

14%	14%	2%	0%
SIMILARITY INDEX	INTERNET SOURCES	PUBLICATIONS	STUDENT PAPERS

PRIMARY SOURCES

1	mafiadoc.com Internet Source	9%
2	nshaucheba.ru Internet Source	3%
3	byanbox.ir Internet Source	2%

Exclude quotes Off
Exclude bibliography Off

Exclude matches < 2%

TABLE OF CONTENTS

1	INTRODUCTION	13
	1.1 Wind Power	13
	1.2 Power Coefficient	14
	1.3 Wind Turbines	15
	1.4 Horizontal Axis and Vertical Axis Wind Turbines:	15
	1.4.1 Vertical Axis Wind Turbines	17
	1.5 Types of VAWTS	18
	1.5.1 Savonius Turbines:	18
	1.5.2 Darrieus Turbines:	19
	1.5.3 Straight Blade Turbines:	21
	1.6 Project Aims and Objectives:	22
2	LITERATURE REVIEW	23
	2.1 Wind Resource and Site Assessment:	23
	2.1.1 Initial Site Identification:	23
	2.2 Analysis of VAWT Performance:	24
	2.2.1 The Disc/Momentum Theory and Betz Limit:	24
	2.3 Aerodynamics of Straight-Blade H-Type Vertical Axis Wind Turbine:	29
	2.4 Double Actuator Disc Theory:	32
	2.5 Multiple Stream-tube Model:	33
	2.6 Double-Multiple-Stream-tube Analysis:	35
	2.7 Computational Fluid Mechanics (CFD) Based Models:	37

3	METHODOLOGY	39
	3.1 VAWT Performance Parameters:	39
	3.1.1 Mass Moment of Inertia:	40
	3.1.2 Tip-Speed Ratio:	40
	3.1.3 Number of Blades:	41
	3.1.4 Turbine Solidity:	41
	3.1.5 Pitch Angle of Blades:.....	41
	3.1.6 Airfoil Type:.....	42
	3.1.7 Turbine Aspect Ratio:	42
	3.1.8 Turbine Swept or Disc Area:.....	43
	3.2 Parametric Study:.....	44
	3.2.1 Airfoil Selection:	44
	3.2.2 Turbine Aspect Ratio:	46
	3.2.3 Turbine Solidity:	49
	3.2.4 Pitch Angle:.....	50
	3.3 Construction of Turbine:.....	51
	3.3.1 Blades:.....	51
	3.3.2 Arms:.....	52
	3.3.3 Hub:.....	52

	3.3.4 Shaft:	53
	3.3.5 Bearings and Bearing Housing:	54
	3.3.6 Tower:	54
	3.3.7 Complete Assembly:	55
	3.4 CFD Analysis:.....	55
4	RESULTS and DISCUSSIONS	58
5	CONCLUSION AND RECOMMENDATION	61
6	Bibliography	62
	APPENDIX I: Property Tables	64
	APPENDIX II: Simulation data	65
	Airfoil Curve Points: X, Y	65
	NACA 0012	65
	NACA 0015	67
	NACA 0018	69
	NACA 0020	71
	NACA 0021	73
	NACA 2412	75
	APPENDIX III: Engineering Drawings.....	78

LIST OF TABLES

Table 1 Aspect Ratios	47
Table 2 Parameters Selected	50
Table 3 Materials	59
Table 4 Final Parameters	60
Table 5 Solidworks Results	77

LIST OF FIGURES

Figure 1 Several typical types of vertical-axis wind turbines: (a) Darrius, (b) Savonius, (c), Solarwind, (d), Helical, (e) Noguchi, (f) Maglev (g) Cochrane [1]	16
Figure 2 Horizontal Axis Wind Turbine [2]	16
Figure 3 Principal embodiment of the Savonius VAWT Patent [1]	19
Figure 4 Images from the Darrius VAWT patent: (a) Curved-Blade rotor embodiment(b) Plane view of Straight-Blade Rotor [1]	20
Figure 5 A Straight-Blade VAWT	21
Figure 6 Wind Velocity Distribution (Pakistan Meteorological Department)	22
Figure 7 Airflow through a Wind Turbine [2]	25
Figure 8 Velocity Profile of Wind Through Turbine	28
Figure 9 VAWT Flow Velocities [3]	29
Figure 10 Double Actuator Disc Theory	32
Figure 11 Steam-Tube Model	34
Figure 12 Plane view of a double-multiple-stream-tube analysis of the flow [1]	35
Figure 13 Numerical Procedure for DMST	37
Figure 14 CFD Solution Steps	38
Figure 15 Pitch Angle of Airfoil	42
Figure 16 Swept Area for Different Turbines	43

Figure 17 NACA Airfoils in Qblade.....	45
Figure 18 Coefficient of Lift Vs Coefficient of Drag in Qblade.....	45
Figure 19 Cl/Cd of Air-Foils.....	46
Figure 20 Turbine Aspect Ratio VS Coefficient of Performance	47
Figure 21 Torque Comparison for Different Aspect Ratios.....	48
Figure 22 Power Vs TSR for Different Rotational Speeds	49
Figure 23 NACA 2412 Blade	51
Figure 24 Arms for Blade Support.....	52
Figure 25 Hub	53
Figure 26 Shaft.....	53
Figure 27 Bearing Housing.....	54
Figure 28 Tower.....	54
Figure 29 Complete Assembly.....	55
Figure 30 Flow Trajectories from Top View	56
Figure 31 Static Analysis in Solidworks.....	56
Figure 32 Total Pressures on Turbine in ANSYS.....	57
Figure 33 Tangential Velocity of Turbine	57
Figure 34 Properties of Air at 1 atm [2].....	64

ABBREVIATIONS

VAWT	Vertical Axis Wind Turbine
HAWT	Horizontal Axis Wind Turbine
DMST	Double Multiple Stream Tube
COP	Coefficient of Power
CFD	Computational Fluid Dynamics

NOMENCLATURE

$K.E$	Kinetic Energy of Air
P_w	Power Available from Air
\dot{m}	Double Multiple Stream Tube
C_p	Coefficient of Power
σ	Turbine Solidity
TSR	Tip-Speed Ratio
α	Angular Acceleration/Angle of Attack
β	Blade Pitch Angle
R	Rotor Radius
A	Turbine Swept Area
c	Chord Length
b	No of Blades
H	Blade Height

1 INTRODUCTION

Pakistan has been facing the energy deficit and load shedding crisis from the time of its independence. Apart from that, the concerns of increasing global warming and harmful emission gases such as CO₂, SO₂, and NO_x, have caused many countries of the world to switch from powerplants that use fossil fuels to renewable energy. Pakistan has a large potential of harvesting energy and decreasing the energy deficiency in the country through wind energy. Wind energy has several advantages over traditional power plants. Wind energy is clean, environmentally friendly, and inexhaustible source, unlike fossil fuels. Currently, most of the wind farms are dominated by HAWTS, but the importance and energy potential of VAWTS cannot be ignored. VAWTS are very small in size than HAWTS and they hardly produce any noise pollution which allows them to be placed near traffic roads and high wind velocity locations.

Soon there is a high chance that the source of fossil fuels may be depleted and, in that case, it is highly recommended to invest in wind energy early on in the 21st century.

1.1 Wind Power

Every object in motion must possess some kind of kinetic energy. High-speed winds in motion contain a large amount of kinetic energy that can be harvested for electricity generation. The kinetic energy of wind can be related as:

$$K.E = \textit{Kinetic Energy} = \frac{1}{2}mv_{\infty}^2$$

Where m is the mass of air under control volume and v_{∞} is the free stream velocity. The rate of energy or power can be obtained by the gradient of kinetic energy.

$$P = \frac{dK.E}{dt} = \frac{1}{2}\dot{m}v_{\infty}^2 \quad (1)$$

The mass flow rate needs to be defined as only a small portion of wind power is converted into useful electrical energy and is dependent on the size of the turbine.

$$\dot{m} = \rho A v_{\infty} \quad (2)$$

Where ρ is the density of air at ambient conditions, A is the area of the windswept normal to the direction of flow.

Now by combining equation (1) and (2) we get,

$$P_w = \frac{1}{2} \rho A v_{\infty}^3 \quad (3)$$

From the investigation of equation (3) we see that to obtain large amounts of power from the wind, we need high swept area, density, and especially the wind velocity because the wind power is proportional to the wind velocity to the third power.

1.2 Power Coefficient

To define the effective efficiency of how much wind power is converted into electrical energy, we define a new term known as the power coefficient. The power from the wind is first used to drive the turbine blades and shaft and hence it is converted to mechanical energy. The mechanical energy is then converted to electrical energy by the use of an alternator and gearbox. The important component of the turbine here is the blades. For the maximum harvest of wind energy, turbine blades are to be carefully designed.

The power coefficient related the conversion of wind power to mechanical energy by the turbine blades and is related as

$$C_p = \frac{P_{Mechanical}}{P_w} \quad (4)$$

Since there are energy losses in the system due to wake, aerodynamic losses, blade-tip vortices, and rotation losses, the power coefficient obtained is very much less than the theoretical value and is usually in the range of 30% to 40%

Lanchester-Betz calculated the theoretical efficiency limit for a Horizontal Axis Wind Turbine which is about 59.3% and is called Betz Limit

For a VAWT however, the limit is about 64% which is determined by momentum, viscous and inviscid theories.

1.3 Wind Turbines

Wind turbines convert wind power into mechanical energy and then into electrical energy. Various types and kinds of turbines have been developed throughout history to harvest free energy from the wind. Each turbine has its pros and cons and the final choice often ends on the most energy for the least price. Wind turbines can be classified into several types, according to their configuration of blades, turbine capacity, generator driving pattern, and location of installation.

1.4 Horizontal Axis and Vertical Axis Wind Turbines:

The most commonly used and found wind turbine today is the Horizontal Axis Wind Turbine. In this type of configuration, the turbine blade is mounted high into the sky on a pedestal. There are very large and usually contain three propellers because a high number of propellers causes high noise pollution. They also need a yaw control system to orient them to the wind. The power generated is restricted by the diameter of the rotor and hence a larger diameter will produce more power but since a HAWT experience large thrust forces and torque, the size is limited by blade strength and construction.

Figure 1 shows several types of Vertical Axis Wind Turbines. The turbine blades of VAWTS rotate about an axis that is normal to the ground. A very important advantage of VAWTS over HAWTS is that they can accept wind from any direction and they do not require any control system to point them in the direction of the wind and thus no yaw control is needed. The turbine construction is also simplified because the main components of the turbine such as gearbox and generator can be located on the ground as compared to HAWTS and as a consequence reduces cost. One limitation of VAWTS is that it requires an external energy source during initiation because it is supported on only one end at the ground and due to buckling and toppling, its practical height is limited. Due to the low amounts of power coefficients of VAWT, their usage is limited and makes a small percentage of the turbines.

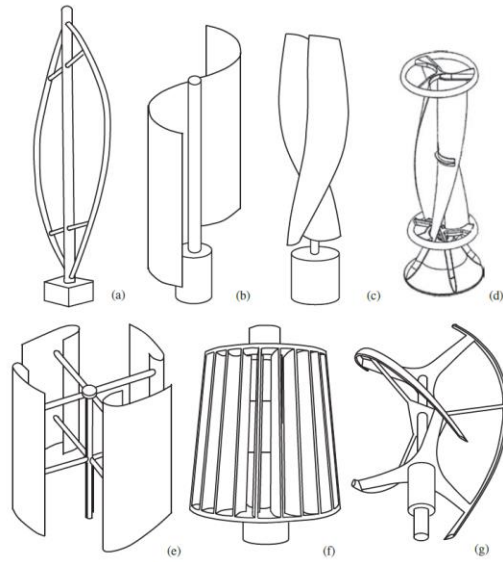


Figure 1 Several typical types of vertical-axis wind turbines: (a) Darrius, (b) Savonius, (c), Solarwind, (d), Helical, (e) Noguchi, (f) Maglev (g) Cochrane [1]



Figure 2 Horizontal Axis Wind Turbine [2]

1.4.1 Vertical Axis Wind Turbines

VAWTs come in a good number of physical configurations and involve some advanced aerodynamics. These turbines were the first ones to be developed and they vary in size according to the requirement of operation. According to literature, the maximum Coefficient of Performance of a VAWT is higher than a HAWT and this makes VAWTs a potential source of energy. From the early 1970s to the 1990s there has been a lot of research on VAWTs and a lot has been learned from that research. Despite the advantages of VAWTs over HAWTS, they have fallen very far behind.

As the VAWTs rotate about an axis normal to ground, the velocity of the air relative to the rotor shaft is changing direction constantly in direction and magnitude. Furthermore, each blade was interacting with the wakes of other blades, and possibly its wakes, when it passes through the downstream half of its path about the turbine axis. Both these effects result in changing aerodynamic forces on the blades, which can lead to a potentially great fatigue issue for the design of the blades and overall turbine structure. The changing blade loads also lead to varying torque transferred to the mechanical load.

The tip speed ratio is a parameter that is very important for a VAWT because most of the designs of VAWTs produce low torques, and even negative torques sometimes at low tip speed ratios. Despite a lot of losses and drawbacks of VAWTs, they are good means of generating electrical energy. There are a variety of sizes of VAWTs available and will vary according to the required application.

1.5 Types of VAWTS

Over the decades, a wide variety of have VAWTs have been developed and they are to be discussed to consider the advantages and efficiency of each. Some of the major types of VAWTs are explained in the next sections.

1.5.1 Savonius Turbines:

The invention credit of this VAWT goes to Savonius, who patented this device in the 1930s. At that time, there was a huge requirement of pumping water in rural or remote areas and the development of wind turbines was used for that purpose. This type of VAWT has been popular both for both professional and amateur types of turbines. Over the years, different variations of Savonius VAWT have been developed and are used to produce electricity. But despite this brilliant innovation, it has never been used in large-scale electricity generation. The Savonius turbine has a low tip to speed ratio has several advantages, such as they produce less aerodynamic noise which is an important issue today in turbines and even for a 3 bladed HAWT. Savonius VAWT provides a cost-effective solution to turbines installed onto the building, but still, a lot of innovations are required to build an efficient integrated wind turbine. Urban types of VAWTS are usually characterized by low wind speeds and high turbulence.

Savonius VAWT is a drag device, with some modifications of the rotor performance available due to air crossing in each vane mutual coupling of the other halves of the rotor. All drag devices have a low operating tip-speed ratio which makes them not a good choice for electricity generation. Mostly, it is used with a gearbox to modify the speed and to minimize the step-up ratio requirement. Several studies have been performed on this type of turbine and it has been determined the coefficient of performance is about 23% at a tip-speed ratio of less than 1. Currently, there have been a lot of studies using CFD analysis also. [1]

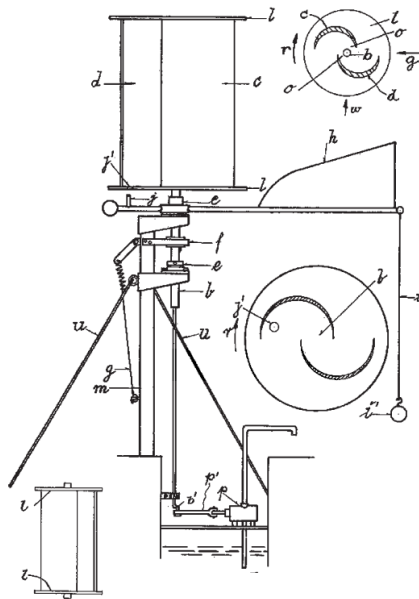


Figure 3 Principal embodiment of the Savonius VAWT Patent [1]

1.5.2 Darrieus Turbines:

The Darrieus VAWT was invented by Darrieus in 1931. This type of turbine had a high tip-speed ratio and it opened up new possibilities of VAWTs in terms of electricity generation. The fundamental principle of this turbine was to increase the velocity of the blades several folds than the free stream velocity of the wind so that the lift forces could be used significantly to improve the coefficient of performance of the VAWTs over previous inventions. This type of VAWT includes both curved blade and straight blade as shown in **Error! Reference source not found**. Darrieus also proposed an active type of straight blades, which could control their pitch, and optimize the angle of attack of air.

There is one drawback of Darrieus VAWT, and that is its self-starting capacity due to insufficient torque to overcome the friction during starting. This is mainly due to very small

lift forces at low rotational speeds of the rotor and mostly for two-bladed- machines, for each of the stationary blades, the torque generated is the same irrespective of the rotor's azimuth relative to the incident wind. In a given wind velocity, the large commercial turbines need to be run at a significantly high tip-speed ratio to avoid rotors from stalling at most azimuth angles. Darrieus VAWT does have some self-starting capability but it is nonetheless not of commercial value.

Some strategies can be used to enhance the self-starting capacity of a turbine. These include:

1. Using an odd number of blades
2. Providing Blade-Pitch Mechanism
3. Using Skewed Blades
4. Increase Solidity

In terms of noise pollution, Darrieus VAWT showed great results as compared to modern HAWTS because of low tip speeds. [1]

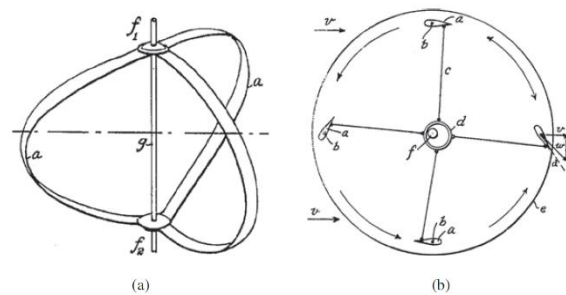


Figure 4 Images from the Darrieus VAWT patent: (a) Curved-Blade rotor embodiment (b) Plane view of Straight-Blade Rotor

[1]

1.5.3 Straight Blade Turbines:

Two of the problems that needed to be addressed in VAWTs were to control the power of the turbine at high wind speeds and active control of the blade pitch resulted in a complex mechanical system for large-scale VAWTs. Musgrove, a British aeronautical engineer, research led to the development of a furling system, whereby straight blades could be hinged at their midpoints so that angle of the blades relative to the axis of the rotor could be adjusted by mechanical actuators. During that time, several geometries were created but it is imperative to mention that the furling method, generates a lot of lift and turbulence which most of cause potential failure of supporting radial arms. A typical design of a straight-blade VAWT is shown in Figure 5.



Figure 5 A Straight-Blade VAWT [1]

1.6 Project Aims and Objectives:

This project aims to design and develop a working H-type straight blade VAWT for areas of good wind speed like Sindh or Punjab to harvest renewable energy and to complete the energy deficit from the country. A wind power density chart and map have been shown in Figure 6, which shows the potential wind energy in different areas of Pakistan. [3]

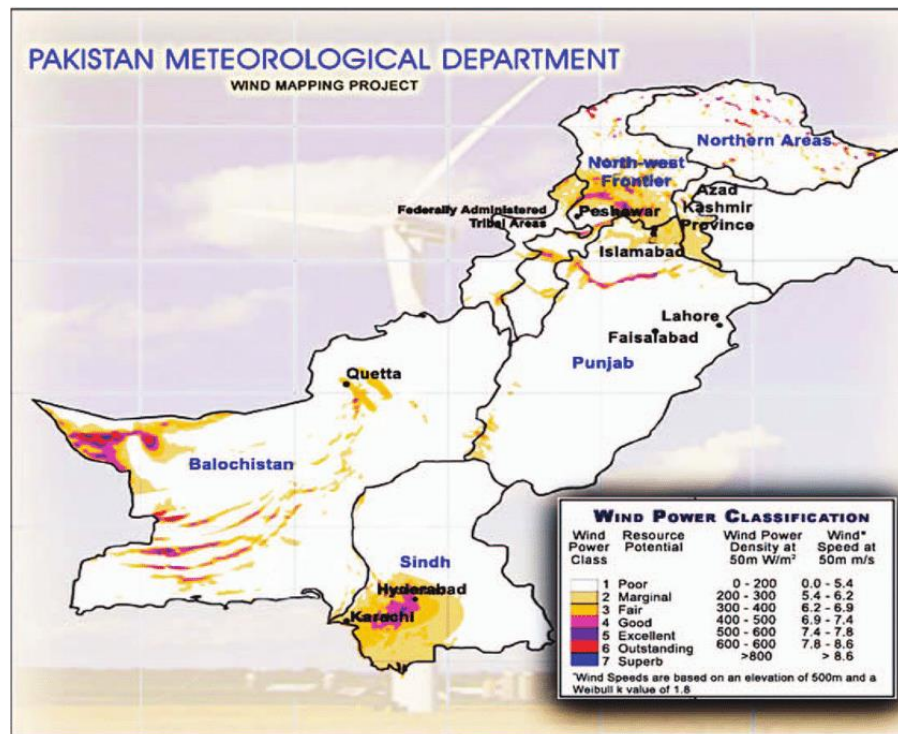


Figure 6 Wind Velocity Distribution (Pakistan Meteorological Department)

2 LITERATURE REVIEW

2.1 Wind Resource and Site Assessment:

Before starting the design of a VAWT, it is imperative to have some information about the potential wind site. The wind map showing the estimate of wind resources in Pakistan is shown in Figure 6. In this section, it will be explained how the wind resource can be assessed. The steps are explained in great detail starting with the identification of the initial site. Later on, different instruments for measuring wind speed are explained. Having analyzed wind data and prepared a layout, the next step is energy yield calculation.

2.1.1 Initial Site Identification:

The wind resource is the most critical aspect to be assessed when planning a wind turbine or a wind farm. The information on the wind climate can be obtained using different approaches and techniques. General information about the wind is mostly available in countries, where wind farms are in vast quantities. The information on wind charts is often color-coded and shows which part of the country has the best wind energy density. The wind analysis is usually produced with Wind Atlas Analysis and Application (WAsP) or combined models which involve the use of both meso and micromodel. The wind data statistics depend on the distance between the target site and the station, the input data, and the complexity of the site itself. The main source of information for wind is usually performed at a height of 10m. These data are based on general models and their accuracy and precision pretty much smaller for wind energy available. A very viable first estimate can be calculated through a nearby wind farm if the production data is available. The

financial success of wind farms depends on the correct assessment of wind resources because wind power is proportional to the third power of wind velocity and hence this step requires maximum possible attention from the designers. But wind measurements are usually neglected and measurement height is not sufficient for the complexity of the site. It cannot be stressed enough that the most expensive part when measuring wind is the loss of data. Any wind resource assessment requires a minimum measurement period of one complete year to avoid seasonal biases. If instrumentation fails due to lightning strike, icing, vandalism, or other reasons and the failure is not spotted rapidly, the lost data

2.2 Analysis of VAWT Performance:

There are several levels of complexity in which one can analyze the performance of VAWTs. There are four main approaches to model the VAWTs and they are:

1. Momentum Models
2. Vortex Models
3. Local Circulation Methods
4. Viscous Models

An extremely basic method that can be used by anyone with basic knowledge of fluid mechanics is disc or blade element momentum theory.

2.2.1 The Disc/Momentum Theory and Betz Limit:

This theory was proposed by Betz in 1926 and It can be used to determine the power, thrust of the wind on an ideal rotor configuration.

In this simple aerodynamic model, the wind turbine is known as the "Actuator Disc Model" in which the rotor is assumed as a homogenous disc that produces energy from the wind.

The following assumption is made in the Actuator Disc Theory:

1. Incompressible Flow
2. Steady-State Flow
3. Frictional Drag is negligible
4. Thrust per unit area is constant over the disc
5. The tangential component of the velocity in the slipstream is zero
6. Continuity of velocity through the disc
7. There is an infinite no of blades in the turbine

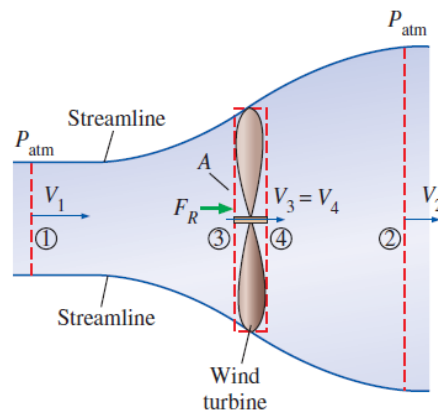


Figure 7 Airflow through a Wind Turbine [2]

We consider two control volumes surrounding the disc area, as shown in Figure 7. The axisymmetric stream tube in Figure 7 can be thought of as an imaginary duct for the airflow through the turbine. From Reynold's Transport theorem, the control volume equations for the momentum of large control volume and steady flow and are analyzed in the x-direction.

$$\frac{dp}{dt} = \frac{d}{dt} \int_{C.V} \rho v dV + \int_{C.S} \rho v \cdot \hat{n} dA \quad (5)$$

Since locations 1 and 2 are far from the turbine, $P_1 = P_2 = P_{\text{atm}}$ which yields zero pressure force on the control volume. The velocities at the inlet and the outlet can be approximated as uniform V_1 and V_2 and the momentum flux correction factors, are $\beta_1 = \beta_2 = 1$. The equation (5) reduces to,

$$F_R = \dot{m}V_2 - \dot{m}V_1 = \dot{m}(V_2 - V_1) \quad (6)$$

The smaller control volume in Figure 7 encloses the turbine and Area $A_3 = A_4 = A$ since the control volume is infinitesimally thin.

Since the air is considered incompressible, $V_3 = V_4$ but since the energy is extracted from the wind from points 3 to 4 then P_3 is not equal to P_4 . By applying momentum equation on the smaller control volume, we get,

$$F_R + P_3A - P_4A = 0 \rightarrow F_R = (P_4 - P_3)A \quad (7)$$

Bernoulli's equation cannot be used in between a turbine due to irrotational flow but it is a good approximation between locations 1 and 3 and between locations 4 and 2.

$$\frac{P_1}{\rho g} + \frac{V_1^2}{2g} + z_1 = \frac{P_3}{\rho g} + \frac{V_3^2}{2g} + z_3 \text{ and } \frac{P_4}{\rho g} + \frac{V_4^2}{2g} + z_4 = \frac{P_2}{\rho g} + \frac{V_2^2}{2g} + z_2 \quad (8)$$

In this ideal analysis, the pressure starts at atmospheric pressure far upstream and rises to P_3 and then drops suddenly to P_4 and then again rises to P_2 ending at $P_2 = P_{\text{atm}}$. Now setting $P_1 = P_2 = P_{\text{atm}}$, $V_3 = V_4$, and $z_1 = z_2 = z_3 = z_4$ and adding equations 6 and 7 we get:

$$\frac{V_1^2 - V_2^2}{2} = \frac{P_3 - P_4}{\rho} \quad (9)$$

By substituting $\dot{m} = \rho V_3 A$ into equation (6) and combining the result with equation (7) and (8)

$$V_3 = \frac{V_1 + V_2}{2} \quad (10)$$

"Then we conclude that the average velocity of the air through an idea wind turbine is the arithmetic average of the far upstream and downstream velocities. The validity of the result of limited by Bernoulli's Equation" [2]

We define a new variable, knows as fraction loss of velocity from far upstream to turbine disc as,

$$a = \frac{V_1 - V_3}{V_1} \quad (11)$$

The velocity through the turbine will become

$$V_2 = V_1(1 - 2a) \quad (12)$$

For an ideal turbine, without irreversible losses such as friction, the power generated by the turbine is just the difference between the incoming and the outgoing kinetic energies.

$$\dot{W}_{ideal} = \dot{m} \frac{V_1^2 - V_2^2}{2} = \rho A V_1 (1 - a) \frac{V_1^2 - V_2^2 (1 - 2a)^2}{2} = 2\rho A V_1^3 a(1 - a)^2 \quad (13)$$

The power coefficient of a turbine is defined as,

$$C_p = \frac{\dot{W}_{rotor\ shat\ ,output}}{\frac{1}{2}\rho V_1^3 A} = \frac{\dot{W}_{ideal}}{\frac{1}{2}\rho V_1^3 A} = \frac{2\rho A V_1^3 a(1 - a)^2}{\frac{1}{2}\rho V_1^3 A} = 4a(1 - a)^2 \quad (14)$$

We can calculate the maximum possible value of C_p by setting the derivative of C_p with respect to a to zero i.e

$$\frac{dC_p}{da} = 0 \quad (15)$$

Equation 15 will yield, $a = 1/3$. Then from equation (14) and $a = 1/3$

$$C_{p,max} = \frac{4}{3} \left(1 - \frac{1}{3}\right)^2 = \frac{16}{27} \approx 0.5926 \quad (16)$$

This is the maximum value of C_p for a HAWT and is known as the Betz limit. All real-world turbines have a maximum power coefficient less than this because we have assumed an ideal scenario and due to losses, turbines never reach this efficiency.

Three effects that lead to a maximum power coefficient less than the Betz limit are,

1. Rotation of the wake behind the rotor
2. A finite number of rotor blades
3. Non-zero aerodynamic drag on the rotor blades

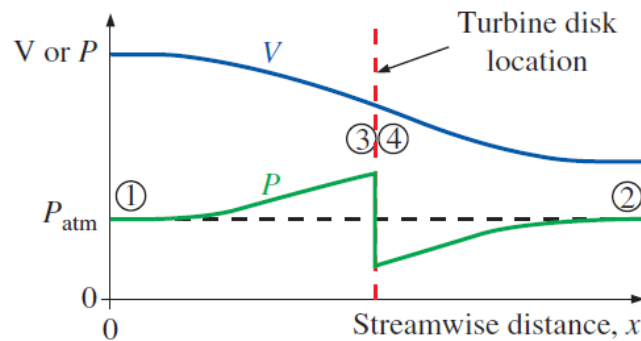


Figure 8 Velocity Profile of Wind Through Turbine [2]

2.3 Aerodynamics of Straight-Blade H-Type Vertical Axis Wind Turbine:

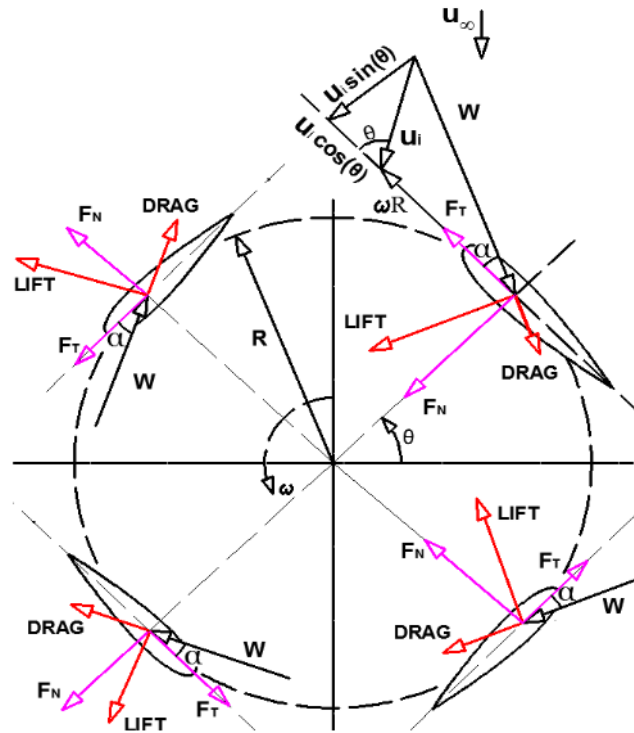


Figure 9 VAWT Flow Velocities [4]

The aerodynamics of this type of VAWT is somewhat complicated than the conventional HAWT because the VAWT has a rotational axis normal to the ground. The main drawbacks of a VAWT are its steep local angle of attacks and turbulent wake coming from the blade upwind.

This type of VAWT works typically at a high tip-speed ratio which makes it a viable option for electricity generation. Unfortunately, they are not self-starting and require some external energy at the start.

From the 2-D representation of VAWT in Figure 9. The relative velocity from the figure can be calculated as:

$$w = \sqrt{(u_i \sin\theta)^2 + (u_i \cos\theta + \omega R)^2} \quad (17)$$

Where u_i is the induced velocity through the rotor, ω is the rotational velocity, and R is the radius of the turbine and θ is the azimuth angle.

It can be also written in non-dimensional form, as

$$\frac{w}{u_\infty} = \sqrt{\left(\frac{u_i}{u_\infty} \sin\theta\right)^2 + \left(\frac{u_i}{u_\infty} \cos\theta + \frac{\omega R}{u_\infty}\right)^2} \quad (18)$$

From equation (10) and (11) we get,

$$u_i = u_\infty(1 - a) \quad (19)$$

Defining a constant λ as

$$\lambda = \frac{\omega R}{u_\infty} \quad (20)$$

Now the equation (18) can be written as,

$$\frac{w}{u_\infty} = \sqrt{((1 - a) \sin\theta)^2 + ((1 - a) \cos\theta + \lambda)^2} \quad (21)$$

The local angle of attack from Figure 9 can be calculated as:

$$\tan\alpha = \frac{u_i \sin\theta}{u_i \cos\theta + \omega R} \quad (22)$$

As we did for relative velocity, we can modify the equation (22) in non-dimensional form, and by using equation (19),

$$\alpha = \tan^{-1} \left(\frac{(1-a)\sin\theta}{(1-a)\cos\theta + \lambda} \right) \quad (23)$$

The normal and tangential force components can be expressed as:

$$C_N = C_L \cos\alpha + C_D \sin\alpha \quad (24)$$

$$C_T = C_L \sin\alpha - C_D \cos\alpha \quad (25)$$

Where C_L and C_D is the lift and drag coefficients respectively for any angle of attack α

Then for a single blade, the normal and tangential forces for a single blade at a single azimuth location are:

$$F_N = \frac{1}{2} \rho w^2 h c C_N \quad (26)$$

$$F_T = \frac{1}{2} \rho w^2 h c C_T \quad (27)$$

Where h is the blade height and c the blade chord length and the product $h*c$ is the wing form area.

The instantaneous thrust force can also be calculated from Figure 9 which is the force of the wind on the turbine experienced by one blade element in the direction of airflow is:

$$T_i = F_T \cos\theta - F_N \sin\theta \quad (28)$$

Using equations (24), (25),(26),(27),(28) we get:

$$T_i = \frac{1}{2} \rho w^2 (h c) (C_N \sin\theta - C_T \cos\theta) \quad (29)$$

The tangential component of force drives the rotation of the wind turbine and produces the necessary torque to generate electricity. The instantaneous torque by a single blade at a single azimuth location is:

$$\tau_i = F_T R \quad (30)$$

Substituting equation (27) into equation (30) we get:

$$\tau_i = \frac{1}{2} \rho w^2 h c C_T R \quad (31)$$

[4]

2.4 Double Actuator Disc Theory:

The main disadvantage of the previous model is its inability to distinguish between the upwind and downwind part of the turbine. Instead of one, two actuators' disks can be placed behind each other connected at the center as shown in Figure 10. Instead of one constant, here we define two constants, a and a' . The induced velocity on the upstream will be the average of the air velocity at far upstream and the air velocity at downstream equilibrium.

The air velocity at the downstream equilibrium can be expressed as:

$$v_e = (2v_i - v_\infty) = (1 - 2a)v_\infty$$

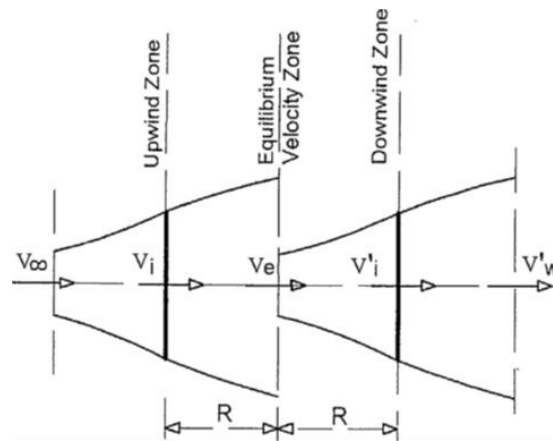


Figure 10 Double Actuator Disc Theory [5]

2.5 Multiple Stream-tube Model:

This model was developed by Strickland and is based on momentum theory. The main improvement as compared to disc models is that more stream tubes make different induced velocities possible as shown in Figure 11. Each stream will have its velocity allowing for a change in the velocity which will depend on the direction, perpendicular to the free stream velocity. The accuracy of this model depends on the number of stream tubes used. The momentum balanced is analyzed for each stream tube separately. For each of the blade elements and stream tubes, the momentum equations have to be calculated and it will result in 'n' induction factors. The total span of the single-stream tube will be divided into multiple tubes by using a fixed angle $\Delta\phi$

$$\Delta\phi = \frac{2\pi}{N_\phi} \quad (32)$$

A single blade passes each stream tube twice per revolution in the upstream and downstream.

The mean aerodynamic thrust with a turbine having “b” blades and spend $\frac{\Delta\phi}{\pi}$ time in the stream tube, we get:

$$T_{mean} = 2 \left(\frac{v\Delta\phi}{\pi} T_i \right) \quad (33)$$

Or a single stream-tube, consider the swept area of the turbine to be $A = HR\Delta\phi$ once can easily get the non-dimensional thrust coefficient

$$C_T = \frac{T_{mean}}{\frac{1}{2} \rho v_{\infty}^2 (HR \Delta \phi \sin \phi)} = \left(\frac{bc}{2R} \right) \left(\frac{w}{v_{\infty}} \right)^2 \frac{2}{\pi} \left(C_t \frac{\cos \phi}{\sin \phi} - C_n \right) \quad (34)$$

The average torque on the rotor by "b" blades and on the complete interval and blade length H is given by:

$$\tau_{avg} = b * \sum_{j=1}^{N_{\phi}} \frac{\left(\frac{1}{2} \rho w^2 H c C_T R \right)}{N_{\phi}} \quad (35)$$

Then the torque coefficient can be defined as:

$$C_{\tau} = \frac{\tau_{avg}}{\frac{1}{2} \rho v_{\infty}^2 HRD} = \left(\frac{Bc}{D} \right) \sum_{i=1}^{N_{\phi}} \frac{\left(\frac{w}{v_{infly}} \right)^2 C_T}{N_{\phi}} \quad (36)$$

$$C_P = C_Q \Lambda \quad (37)$$

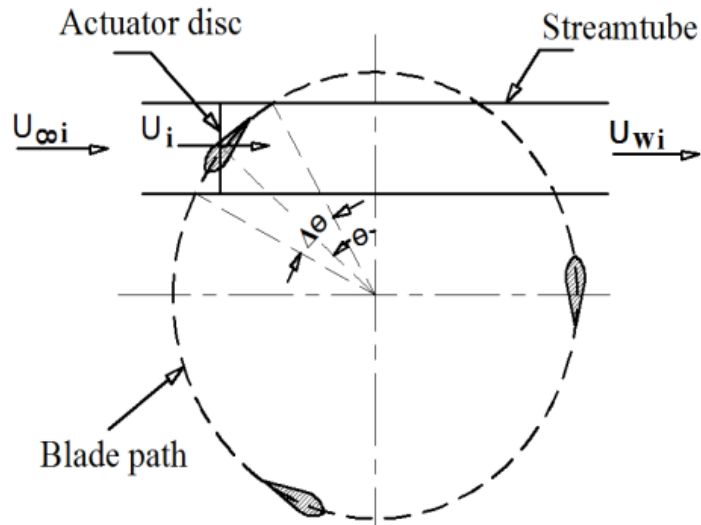


Figure 11 Steam-Tube Model [4]

2.6 Double-Multiple-Stream-tube Analysis:

In the previous models, the performance of VAWT was estimated by using momentum analysis and the level of difficulty was fairly simple in which single or multiple stream-tubes were considered. However, for accurate analysis, it is preferable to use multiple stream tube analysis since the resultant wind velocities and wind forces are strong functions of azimuth angle.

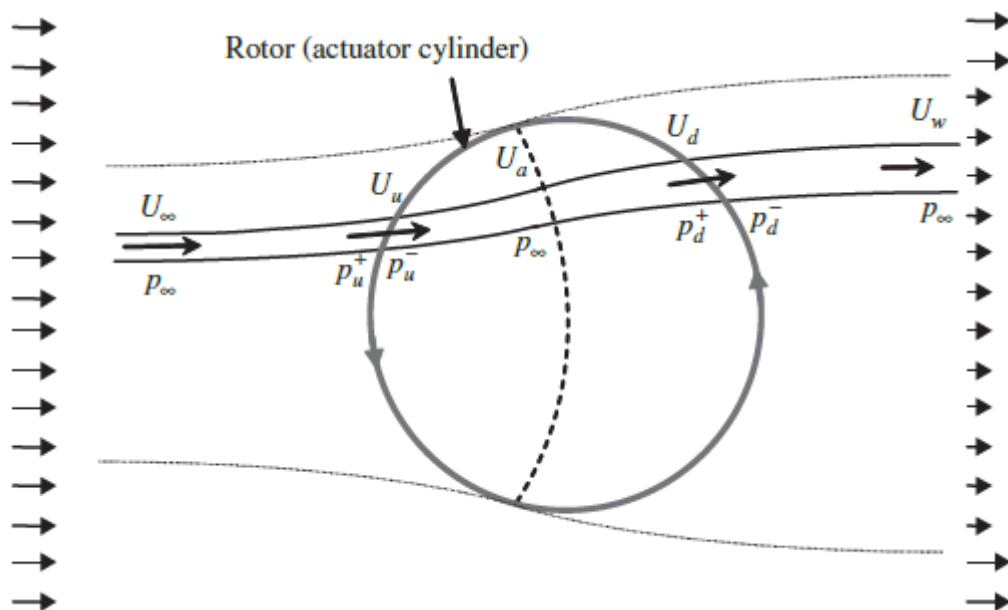


Figure 12 Plane view of a double-multiple-stream-tube analysis of the flow [1]

The Double-Multiple Stream Tube-Model was patented by Loth and McCoy in 1983. Later on, Paraschivoiu and Delclaux combined the multiple stream-tube theory with the double actuator disc theory. This theory will allow us to model velocity variations in the direction normal to the free-stream velocity.

The previous models were not able to calculate the influence of upwind on the downwind part of the turbine. The blades extract energy from the wind and the wind speed downstream is less than the wind speed at far upstream.

The interaction of the turbine with air upstream and downstream are treated separately.

The assumption in this model is that the wake from the upstream pass is fully expanded and the maximum wake velocity has been reached before the interaction with the blades in the downstream. Then the downstream velocity will see a reduction in velocity.

The Double-Multiple-Stream tube model simultaneously solves two equations for the stream-wise force at the actuator disc, one obtained by conservation of momentum and the other based on the aerodynamic coefficients of the airfoil (lift and drag) and the local wind velocity. These equations are solved twice; for the upwind and the downwind part of the rotor.

The thrust coefficient, torque coefficient, and power coefficient can be calculated once the relative wind velocity and angle of attack are found in the new induction method.

The DMST model requires numerical methods and calculations to solve the induction factor equation.

The following procedure is followed to calculate the flow velocity in DMST.

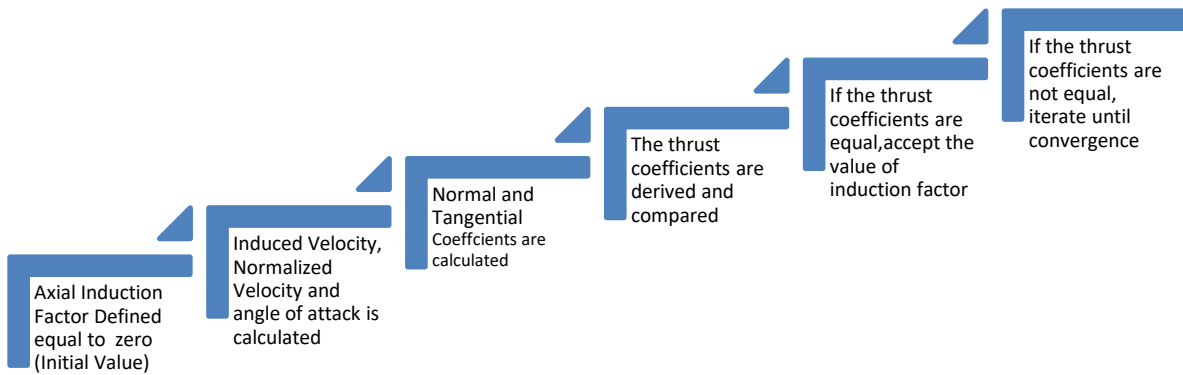


Figure 13 Numerical Procedure for DMST

One of the popular open-source software that is used for this model is named Qblade.

2.7 Computational Fluid Mechanics (CFD) Based Models:

The importance of computer-aided analysis cannot be ignored as modern software are capable of performing sophisticated analysis. CFD and experimental analysis can be performed to assess the accuracy of the results and whether the results complement each other or not. For example, engineers may obtain global properties, such as lift, drag, pressure drop, or power, experimentally, but use CFD to obtain details about the flow field, such as shear stresses, velocity, and pressure profiles, and flow streamlines. [6]

The procedure for CFD analysis is summarized below:

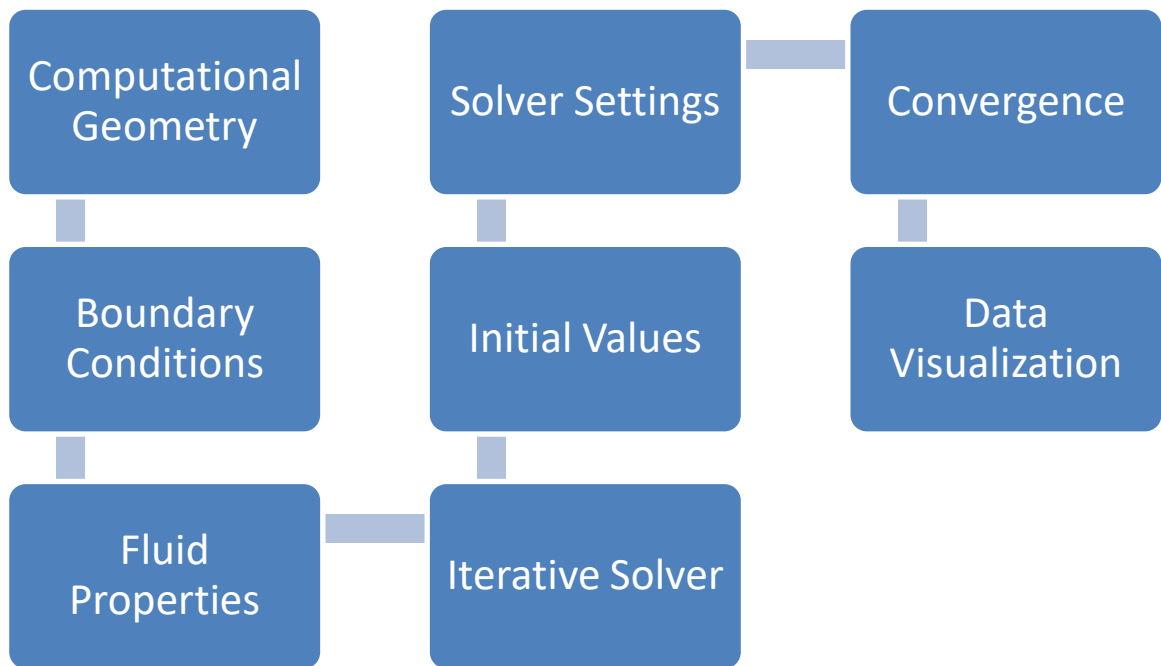


Figure 14 CFD Solution Steps

3 METHODOLOGY

In this section, we will design the straight-blade H-type VAWT by first using parametric performance analysis, and then comes the design analysis. Following steps will be followed for the design of VAWT:

1. **Performance Analysis:** Study of different parameters that will affect the performance. Using this step, we will get the overall dimensions of the turbine.
2. **Design Analysis:** In this step, the material will be selected by the knowledge of forces from the previous step and stress analysis.

3.1 VAWT Performance Parameters:

The parameters that would affect the different design aspects and performance of the VAWT are:

1. Mass Moment of Inertia
2. Tip-Speed Ratio
3. Number of Blades
4. Turbine Solidity
5. Pitch Angle of Blades
6. Airfoil Type
7. Turbine Aspect Ratio
8. Turbine Swept or Disc Area

Each of the performance parameters is explained in detail in this section.

3.1.1 Mass Moment of Inertia:

Moment of inertia has a big effect on the performance of the VAWT because it is proportional to torque necessary or electricity generation. Hence a VAWT with a lower value of the moment of inertia will spin faster and generate greater electricity. But by reducing the moment of inertia, the stability is somewhat reduced at high wind speeds.

From rotational mechanics, we know that,

$$\alpha = \frac{\tau}{I_m} \quad (38)$$

Where α is the angular acceleration, τ is the aerodynamic torque and I_m is the mass moment of inertia of the turbine.

3.1.2 Tip-Speed Ratio:

Another important design factor in VAWT is its tip-speed ratio. It is defined as the ratio of the rotational or tangential speed of the turbine to the free-stream velocity of the wind.

$$\text{Tip - Speed Ratio} = \frac{\omega R}{v_\infty} \quad (39)$$

The tip-speed ratio should be optimized because if the rotational speed is too high, then it will block the incoming air and reduce any useful power extraction from the wind. The same thing occurs if the rotational speed is low and that would mean that the wind just passes the turbine without any useful power extraction.

3.1.3 Number of Blades:

The number of blades in a VAWT has a direct effect on the fluctuation of torque that is being generated. Good performance was shown with a VAWT that had an odd number of blades as compared to an even number of blades. The smooth operation is required in a VAWT design and it is economical to go with a design that was three blades.

3.1.4 Turbine Solidity:

An important non-dimensional parameter that determines and affects the self-starting capabilities of a VAWT and is defined as the ratio of blade plane-form area to projected Turbine Area.

$$\sigma = \frac{bc}{R} \quad (40)$$

Solidity will determine whether the assumptions in momentum models are applicable or not. A self-starting turbine is achieved only when $\sigma \geq 0.4$ [1]

3.1.5 Pitch Angle of Blades:

For maximum performance, the proper selection of airfoil is necessary and it will greatly affect the aerodynamic performance. It is difficult to compromise the turbine solidity, power coefficient when it comes to the selection of airfoil.

Pitch angle has a great impact on the overall performance of VAWT. The different pitch angles can increase the coefficient of power and that is why different pitch control mechanisms are used.

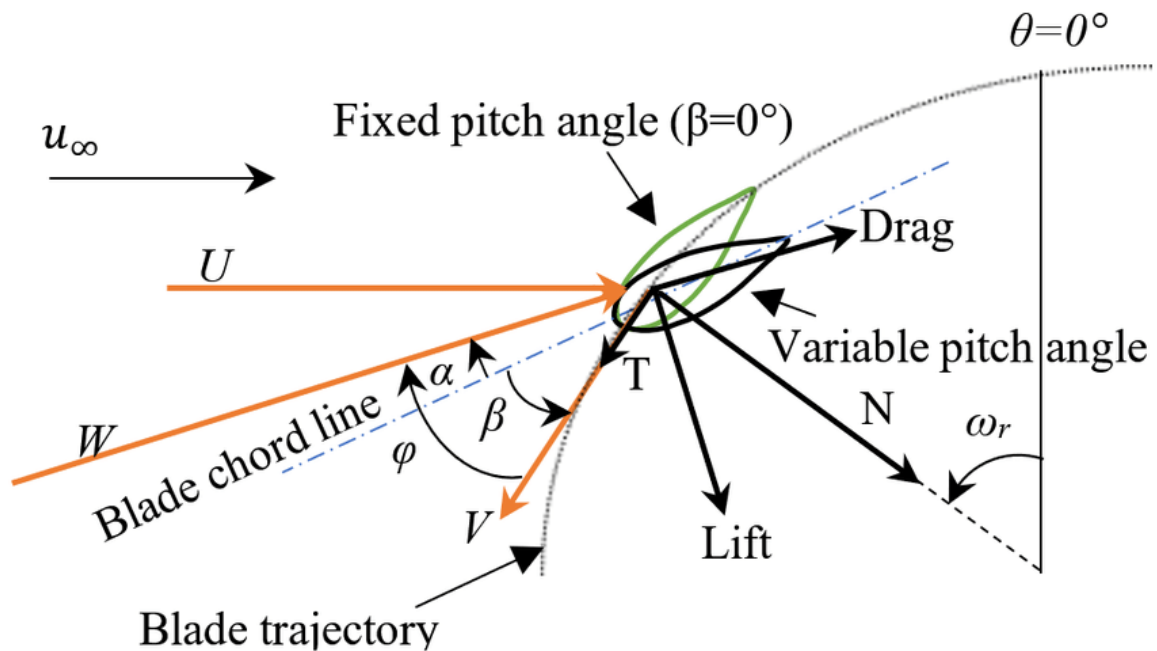


Figure 15 Pitch Angle of Airfoil [7]

3.1.6 Airfoil Type:

It is really important to analyze different airfoil types and based on the best performance, the airfoil type then is selected. The following factors may be used to weigh different airfoils.

1. Power Coefficient
2. Lift/Drag Ratio
3. Symmetry
4. Structural Integrity

3.1.7 Turbine Aspect Ratio:

Turbine-Aspect ratio is defined as the ratio of turbine blade height to the turbine rotor radius. This ratio changes Reynold's number and Reynold's number has a direct effect on

the coefficient of power. A high aspect ratio means greater rotational velocity than aerodynamic torque for the same power produced.

3.1.8 Turbine Swept Area [8]r Disc Area:

It is the projected area normal to airflow for which the air passes through the turbine. The area will depend on the rotor configuration and some of them are shown in Figure 16. For a HAWT the swept area is circular shaped.

Swept area is related to the coefficient of performance and mass flow rate and is adjusted by the dimensions of the VAWT.

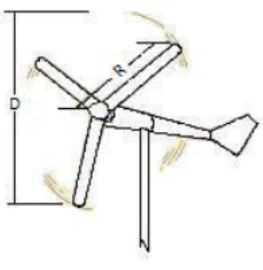
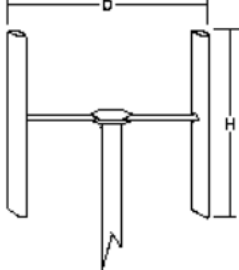
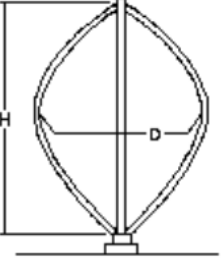
Rotor blade configuration			
	Conventional rotor	H-rotor	Darrieus rotor
Swept Area	$A = \pi R^2$	$A = DH$	$A = 0.65DH$

Figure 16 Swept Area for Different Turbines [8]

3.2 Parametric Study:

Initially, we will define some parameters for the turbine and analyze the results using equations and literature described in the previous sections.

From Figure 6 we can see that the average wind velocity in Punjab is about 8 m/sec and we have assumed that the air is at room temperature. From APPENDIX I: Property Tables, the density of air at 25°C is 1.184 kg/m³

$$P = \frac{1}{2} \rho A v^3 \quad (41)$$

Based on our CAD Models, the Height of the blade is $H = 1.45$ m, and the diameter of the rotor is 1.5 m and hence the swept area is 2.175 m².

The maximum power that can be extracted from these dimensions and wind velocity is:

$$P = \frac{1}{2} * 1.184 * 2.175 * 8^3 = 659.25 \text{ W} \quad (42)$$

We also said that the maximum efficiency of a VAWT is about 64% (pg.14) then the maximum power that can be obtained is, about 421.9 W.

The power obtained will increase with wind velocity as it is proportional to its third power and during storms, a very huge amount of power can be obtained.

3.2.1 Airfoil Selection:

Qblade software has been used to analyzed different kinds of NACA Airfoils. First, the airfoils were modeled in the software, and then they were analyzed at about 10⁵ Reynold's Number. Different results were obtained for the coefficient of lift and drag.

The simulation and airfoil data has been given in APPENDIX II: Simulation data

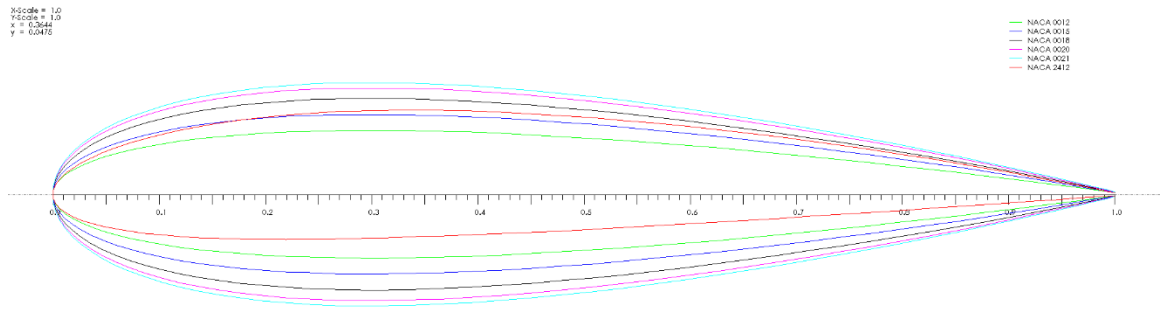


Figure 17 NACA Airfoils in Qblade

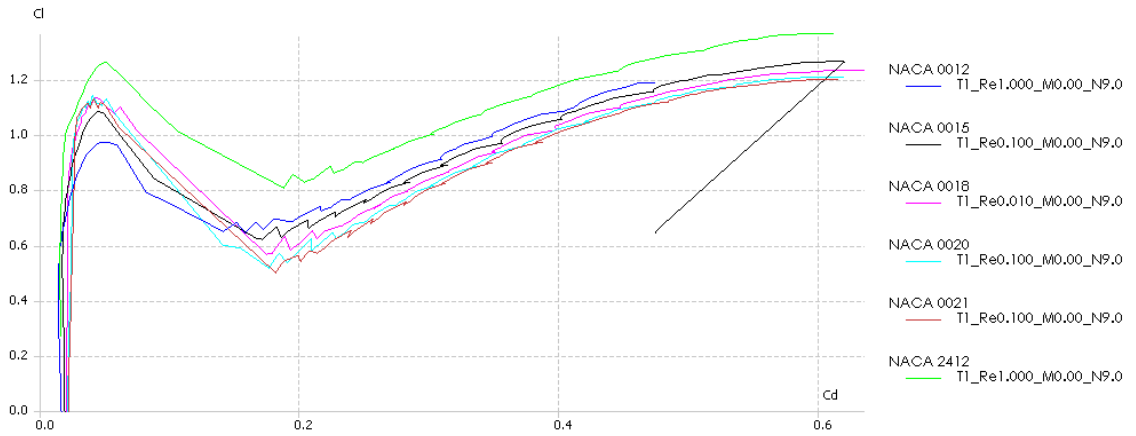


Figure 18 Coefficient of Lift Vs Coefficient of Drag in Qblade

At a different angle of attacks, the Qblade software was used to compare the different airfoils, as we can see from Figure 18, NACA 2412 has the most amount of lift and least amount of drag at all angles of attacks.

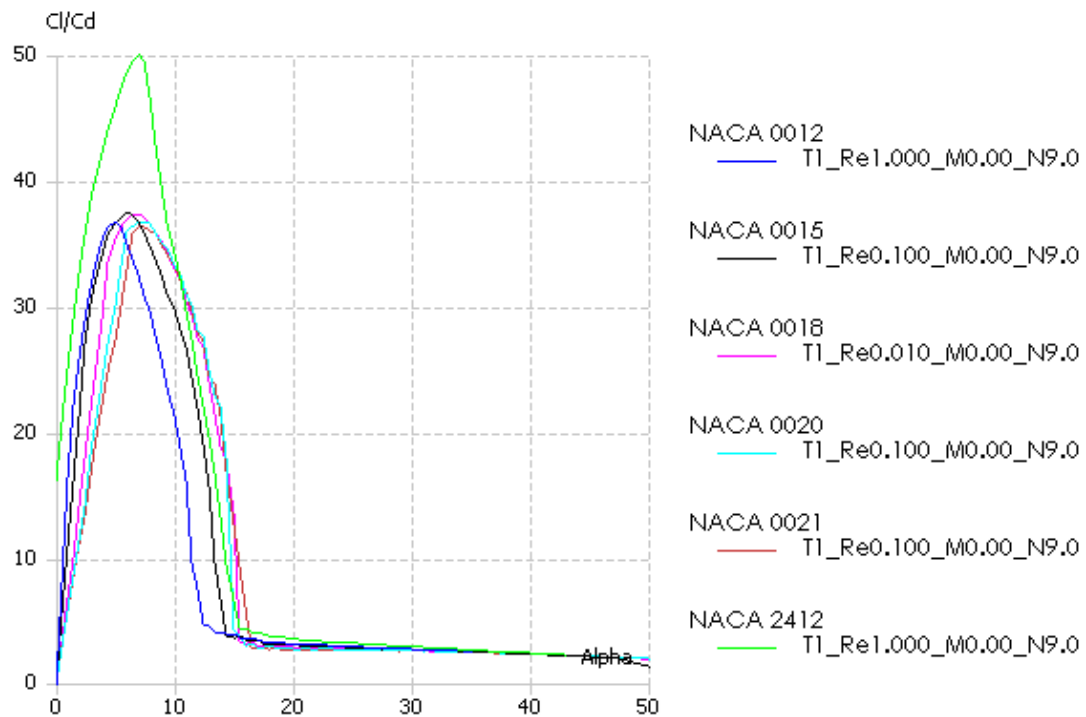


Figure 19 Cl/Cd of Air-Foils

The maximum lift to drag ratio was obtained at about a 7.5° angle of attack.

3.2.2 Turbine Aspect Ratio:

Having selected the airfoil from the previous section, the turbine aspect ratio is to be compared next. Different aspect ratios were compared and the best aspect ratio was chosen or the maximum coefficient of performance.

Following parameters were used in Qblade for the comparison of different aspect ratios.

Table 1 Aspect Ratios

Turbine Height (m)	Rotor Radius (m)	Aspect Ratio (H/R)	Chord Length (m)
1.45	1.5	0.97	0.25
2.5	1.5	1.67	0.25
3.5	1.4	2.86	0.25
4.5	1.2	3.75	0.25
6	1	6	0.25

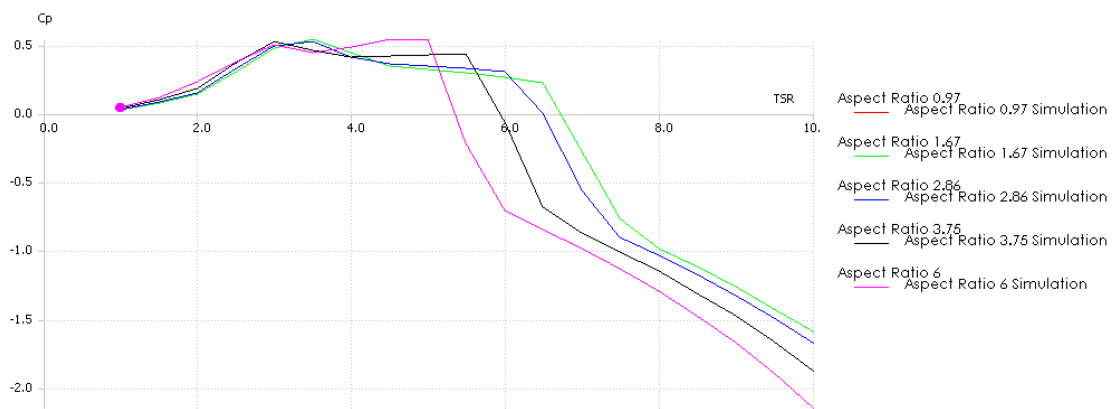


Figure 20 Turbine Aspect Ratio VS Coefficient of Performance

From Figure 20 we see that the maximum coefficient of performance is achieved for the aspect ratio of 6, but we have chosen an aspect ratio of 3.75 because the bigger aspect ratio would cost more and we cannot just make our decision based on power coefficient, we also need to see the torque generated as shown in

With an aspect ratio of 3.75 and NACA 2412, a power coefficient of 0.527 is achieved.

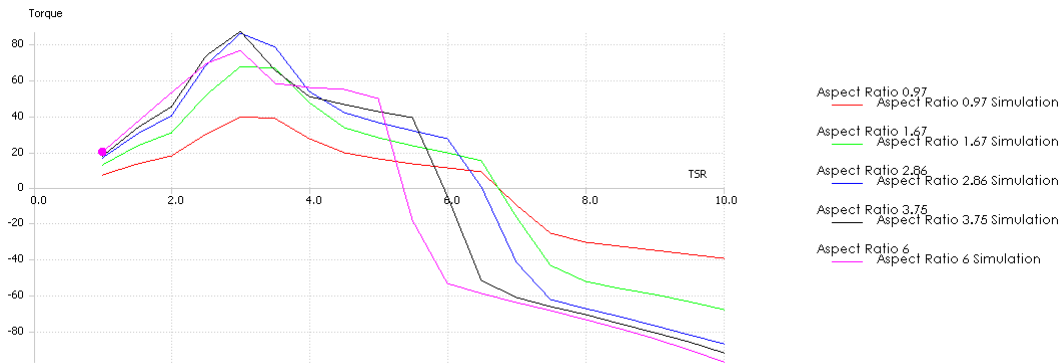


Figure 21 Torque Comparison for Different Aspect Ratios

The maximum torque is achieved for an aspect ratio of 3.75 and the power coefficient is also good. The torque achieved by the aspect ratio 3.75 is about to 86 N.m at about 3 Tip-Speed Ratio.

The Qblade performs calculations based on the DMST model explained in the literature.

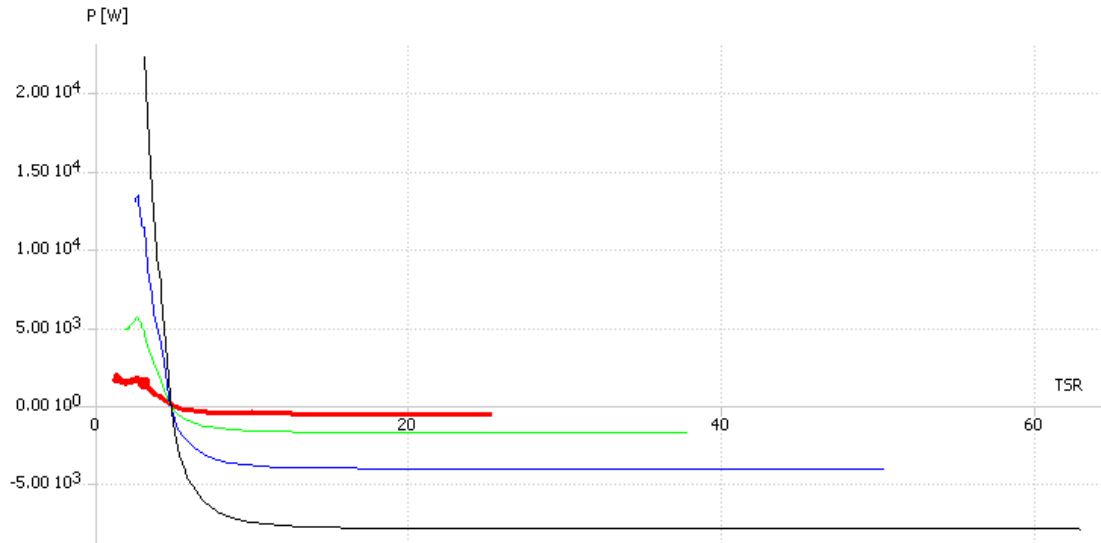


Figure 22 Power Vs TSR for Different Rotational Speeds

Figure 22 compares the power being generated at different Tip-speed ratios and different rotational speeds. The red line shows an rpm of 200. At this point using equations(3) the maximum power that can be achieved for an aspect ratio of 3.75 is 1627 W for a wind speed of 8 m/sec.

3.2.3 Turbine Solidity:

For an aspect ratio of 3.75, the turbine height is 4.5 meters and its rotor radius is 1.2 m and the no of blades are 3. Then the solidity is,

$$\sigma = \frac{bc}{R} = \frac{3 \cdot 0.25}{1.2} = 0.625 \quad (43)$$

As discussed in the literature, for a self-starting turbine, the solidity should be greater than 0.4.

3.2.4 Pitch Angle:

Although the power coefficient is affected by the pitch angle it is not as significant as the other variables and hence a 0° fixed pitch angle is used.

The overall dimensions calculated in this section that will be used in the next section are:

Table 2 Parameters Selected

Turbine Swept Area (m ²)	5.4
Turbine Rotor Diameter (m)	1.2
Blade Length (m)	4.5
Number of Blades	3
Solidity (m)	0.625
Chord Length (m)	0.25
Tip-Speed Ratio	3
Airfoil Type	NACA 2412
Fixed Pitch Angle (Degree)	0

3.3 Construction of Turbine:

Having selected basic dimensions and parameters from the previous section, CAD models were made and its construction is explained here. Further dimensions can be seen from the drawing in APPENDIX III: Engineering Drawings

3.3.1 Blades:



Figure 23 NACA 2412 Blade

As seen in parametric analysis, for an aspect ratio of 3.75, the blade height is about 4.5 m and its cord length is 251mm. We have used NACA 2412 airfoil to construct the blade in Solidworks. A transparent view of the blade is shown in Figure 23 and we have used ribs to spars to add some structural strength to the wind.

3.3.2 Arms:

The arms are used to support the blades to the tower and to rotate the shaft. Based on our parametric calculations, the rotor radius was used to be 1.2 m. The blades are attached to arms using bolts. The arms are shown in Figure 24



Figure 24 Arms for Blade Support

3.3.3 Hub:

The hub supports the bearings and bearing housings and the shaft. The arms are also supported by the hub.

The hub is made out of steel and has a good height and because of that, it is quite heavy.



Figure 25 Hub

3.3.4 Shaft:

The shaft is connected to the bearing and the arms and can be attached to a gearbox and generator for electricity generation

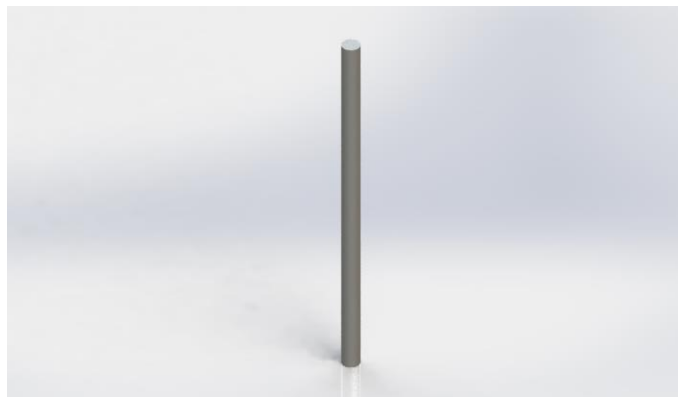


Figure 26 Shaft

3.3.5 Bearings and Bearing Housing:

The bearing housing is supported by the hub and SKF bearings are attached to the housing.

The housing is bolted to the tower on the lower end.



Figure 27 Bearing Housing

3.3.6 Tower:

The tower supports all the weight and is made in a flange type so that it can be fastened to the concrete using bolts.



Figure 28 Tower

3.3.7 Complete Assembly:

The complete assembly is shown in Figure 29

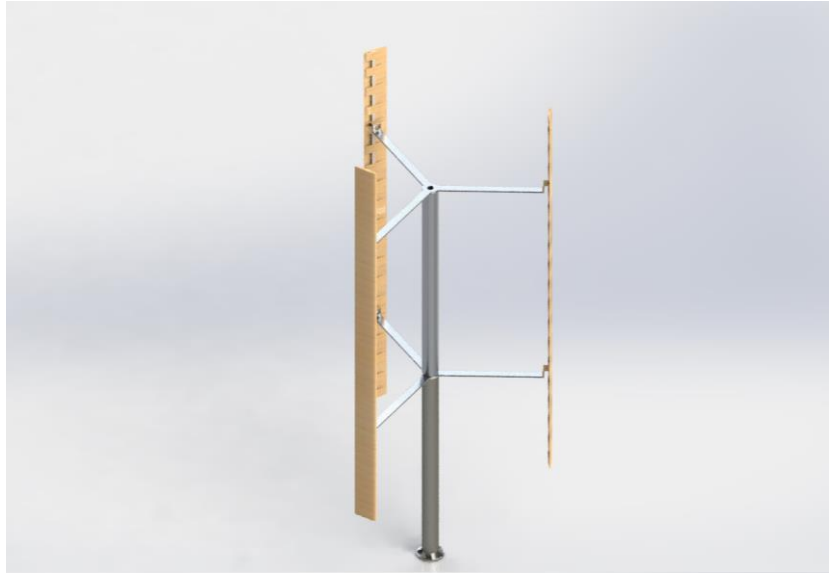


Figure 29 Complete Assembly

3.4 CFD Analysis:

Initial CFD analysis was performed in Solidworks to investigate the flow trajectories and the coefficient of performance at 200 rpm and 8 m/sec wind velocity. From Figure 30 we see that there is a small vortex inside the wind turbine which may cause a slight decrease in performance due to reverse flows.

A 0.4 coefficient of power was obtained based on torque calculations by Solidworks and wind velocity.

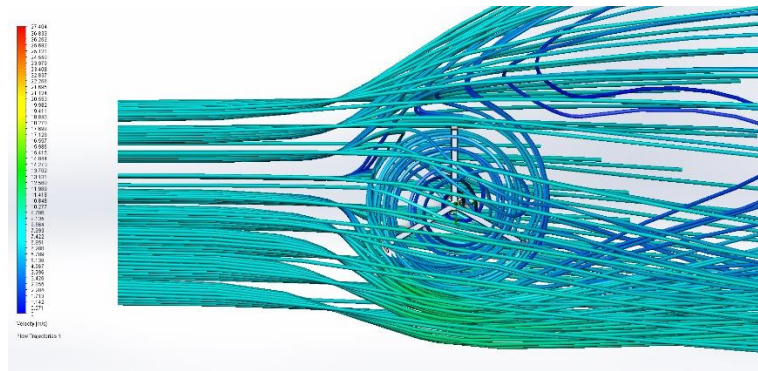


Figure 30 Flow Trajectories from Top View

The pressures from CFD analysis were imported into solid works static analysis. Based on our CFD analysis, the stress is shown in Figure 31.

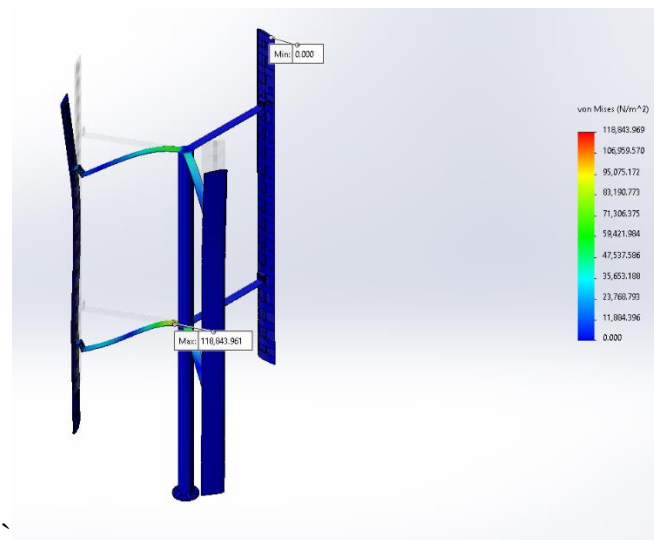


Figure 31 Static Analysis in Solidworks

The maximum von mises stress was obtained at about 118 kPa and it is was below the yield point of any material.

A similar simulation was run in ANSYS but a 6 DOF 2d model was used for simplification of results.

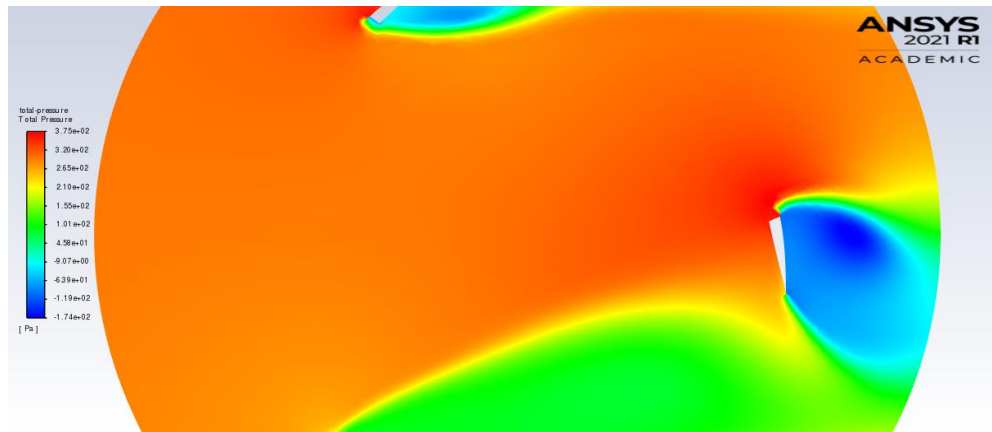


Figure 32 Total Pressures on Turbine in ANSYS

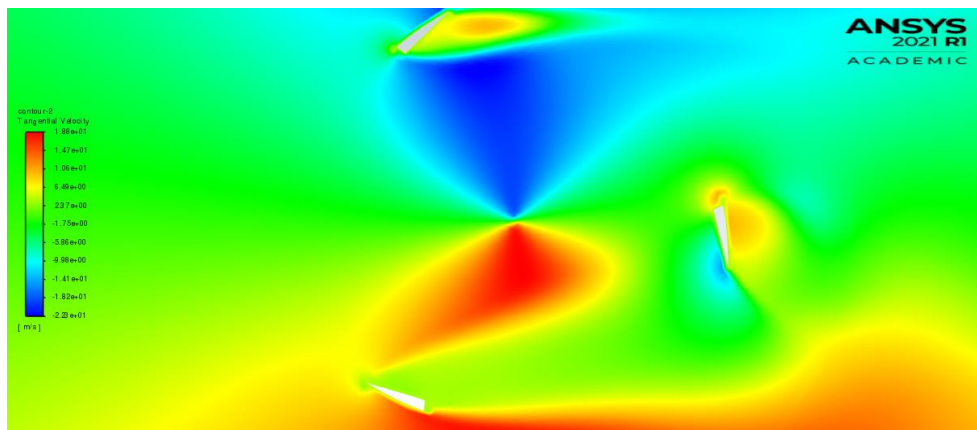


Figure 33 Tangential Velocity of Turbine

A moving mesh method was used to obtain the tangential velocity of the blade at 200 rpm.

4 RESULTS AND DISCUSSIONS

In the previous section, we had performed many simulations and analyses. We first defined some performance parameters and using Qblade, we selected airfoil and some of the parameters of VAWT. We then performed CFD in Solidworks and ANSYS to verify our results. Based on the pressures on the turbine, we also performed static simulations and we have selected the following materials for each part of the turbine based on the results.

The results obtained are based on the DMST model that was implemented using Qblade software and based on the comparative results obtained using DMST model, different geometry was analyzed for the best performance i.e., different airfoils, different aspect ratios etc.

Calculation involved do not account or any losses due to vortex generation and turbulence so the real performance of the turbine will be less than the explained in the previous sections.

During the calculations and simulations, the turbine was limited to the wind speeds that are usually available in Islamabad or Pakistan but in no the turbine is restricted to higher wind speeds in fact greater wind speeds is a plus for power generation but too much speed can damage the turbine and a thresh hold has to be set or braking mechanism is to be used for high wind speeds.

The materials chosen for the turbine are a product of different analysis and on the basis of structural integrity and cost. The blades are made from balsa wood as it is strong and very light which is a center of attraction for our VAWT.

Table 3 Materials

Part Name	Material	Selection Criteria	Elastic Modulus	Yield Strength	Weight
Blade Spar	Plywood	High Strength	8.62 GPa	63 Mpa	1.8 kg
Blade Ribs	Balsa Wood	Low Weight	3 Gpa	20 Mpa	45g
Blade Body	Balsa Wood	Low Weight	3 Gpa	20 Mpa	3.2 kg
Arms	6063-T6 Aluminum	Bending Strength	69 Gpa	215 Mpa	9.6 kg
Hub	2014 Alloy Aluminum	Torsional Stiffness	73 Gpa	96 Mpa	122.65 kg
Shaft	AISI 1045 Steel, cold drawn	Torsional Stiffness	205 Gpa	530 Mpa	53.27 kg
Towe Base	AISI 1045 Steel, cold drawn	Overall Strength and Mass Density	205 Gpa	530 Mpa	412.20 kg

Based on our previous analysis, we have come to the following quantities and dimensions:

Table 4 Final Parameters

Quantity	Value
Turbine Swept Area (m ²)	5.4
Turbine Diameter (m)	1.2
Blade Length (m)	4.5
Number of Blades	3
Solidity	0.625
Chord Length (m)	0.25
Tip-Speed Ratio	3
Airfoil Type	NACA 2412
Fixed Pitch Angle (Degree)	0
Maximum Coefficient of Power	0.527

5 CONCLUSION AND RECOMMENDATION

We first discussed the historical development of the VAWT and how VAWT has several advantages over HAWT. We also discussed the types of VAWTs and their pros and cons. The literature related to turbines and VAWT specifically was reviewed. We also derived the maximum coefficient of power for HAWT and also stated COP for VAWT. Firstly, we went over the necessity of site assessment and identification for the installment of VAWT and we also went over instruments that are used to measure average wind velocity. The wind density map of Pakistan was also reviewed to determine the average wind velocity in Pakistan. We also reviewed the aerodynamics and forces developed on the turbine blade and based on that we derived some useful equations and parameters. We defined our methodology that we will analyze firstly the performance parameters that will affect the efficiency of the turbine and coefficient of power. We performed our parametric study using DMST which was implemented in Q-Blade software. Using Q-blade, we also compared different airfoils to be in VAWT, and based on the maximum torque, coefficient of lift, and COP, we selected NACA 2412 airfoil. We also selected the aspect ratio for maximum COP for this airfoil. With the initial dimensions and parameters fixed, we developed a CAD model of VAWT. After CAD models were made, CFD analysis was performed to investigate the flow trajectories, COP, and pressure on the VAWT.

CFD study results were imported into a static study to determine the stresses generated in the VAWT. Based on the CFD and structural analysis finally, materials were selected.

In the end, all the parameters and selected dimensions were summarized in the table.

6 BIBLIOGRAPHY

- [1] W. Tong, Wind Power Generation and Wind Turbine Design, WIT Press, 2010.
- [2] J. M. C. Yunus A. Cengel, Fluid Mechanics, Fundamentals and Applications, MCGrawHill, 2013.
- [3] Tauseef Aized, Syed Muhammad Sohail Rehman et al, "Design and analysis of wind pump for wind conditions in Pakistan," *Advances in Mechanical Engineering*, vol. 9, no. 11, 2019.
- [4] Asress Mulugeta Biadgo, Aleksandar Simonovic et al, "Numerical and Analytical Investigation of Vertical Axis Wind Turbine," *FME Transactions*, pp. 49-58, 2013.
- [5] E. Saber, Rehab Afify and Hesham Elgamal, "Performance of SB-VAWT using a modified double multiple streamtube model," *AEJ - Alexandria Engineering Journal*, vol. 57, no. 4, 2018.
- [6] Adair, Zhumabay Bakenov and Martin Jaeger, "Building on a Traditional Chemical Engineering Curriculum Using Computational Fluid Dynamics," *Education for Chemical Engineers*, vol. 9, no. 4, 2014.
- [7] Gebreel Abdalrahman, William Melek et al, "Pitch angle control for a small-scale Darrieus vertical axis wind turbine with straight blades (H-Type VAWT)," *Renewable Energy*, vol. 114, no. B, pp. 1353-1362, 2017.

- [8] Phillip Koko and Kanzumba Kusakana, "TECHNO-ECONOMIC ANALYSIS OF AN OFF-GRID MICRO-HYDROKINETIC RIVER SYSTEM AS A REMOTE RURAL ELECTRIFICATION OPTION," 2015.
- [9] Ahmed El. Attar and Ahmed Shahin, "Vertical Axis Wind Turbine," Alexandria University, 2018.
- [10] David Marten, "QBlade v0.95 Guidelines for Lifting Line Free Vortex Wake Simulations".

APPENDIX I: PROPERTY TABLES

TABLE A-9							
Properties of air at 1 atm pressure							
Temp. $T, ^\circ\text{C}$	Density $\rho, \text{kg/m}^3$	Specific Heat c_p J/kg·K	Thermal Conductivity $k, \text{W/m}\cdot\text{K}$	Thermal Diffusivity $\alpha, \text{m}^2/\text{s}$	Dynamic Viscosity $\mu, \text{kg/m}\cdot\text{s}$	Kinematic Viscosity $\nu, \text{m}^2/\text{s}$	Prandtl Number Pr
-150	2.866	983	0.01171	4.158×10^{-6}	8.636×10^{-6}	3.013×10^{-6}	0.7246
-100	2.038	966	0.01582	8.036×10^{-6}	1.189×10^{-6}	5.837×10^{-6}	0.7263
-50	1.582	999	0.01979	1.252×10^{-5}	1.474×10^{-5}	9.319×10^{-6}	0.7440
-40	1.514	1002	0.02057	1.356×10^{-5}	1.527×10^{-5}	1.008×10^{-5}	0.7436
-30	1.451	1004	0.02134	1.465×10^{-5}	1.579×10^{-5}	1.087×10^{-5}	0.7425
-20	1.394	1005	0.02211	1.578×10^{-5}	1.630×10^{-5}	1.169×10^{-5}	0.7408
-10	1.341	1006	0.02288	1.696×10^{-5}	1.680×10^{-5}	1.252×10^{-5}	0.7387
0	1.292	1006	0.02364	1.818×10^{-5}	1.729×10^{-5}	1.338×10^{-5}	0.7362
5	1.269	1006	0.02401	1.880×10^{-5}	1.754×10^{-5}	1.382×10^{-5}	0.7350
10	1.246	1006	0.02439	1.944×10^{-5}	1.778×10^{-5}	1.426×10^{-5}	0.7336
15	1.225	1007	0.02476	2.009×10^{-5}	1.802×10^{-5}	1.470×10^{-5}	0.7323
20	1.204	1007	0.02514	2.074×10^{-5}	1.825×10^{-5}	1.516×10^{-5}	0.7309
25	1.184	1007	0.02551	2.141×10^{-5}	1.849×10^{-5}	1.562×10^{-5}	0.7296
30	1.164	1007	0.02588	2.208×10^{-5}	1.872×10^{-5}	1.608×10^{-5}	0.7282
35	1.145	1007	0.02625	2.277×10^{-5}	1.895×10^{-5}	1.655×10^{-5}	0.7268
40	1.127	1007	0.02662	2.346×10^{-5}	1.918×10^{-5}	1.702×10^{-5}	0.7255
45	1.109	1007	0.02699	2.416×10^{-5}	1.941×10^{-5}	1.750×10^{-5}	0.7241
50	1.092	1007	0.02735	2.487×10^{-5}	1.963×10^{-5}	1.798×10^{-5}	0.7228
60	1.059	1007	0.02808	2.632×10^{-5}	2.008×10^{-5}	1.896×10^{-5}	0.7202
70	1.028	1007	0.02881	2.780×10^{-5}	2.052×10^{-5}	1.995×10^{-5}	0.7177
80	0.9994	1008	0.02953	2.931×10^{-5}	2.096×10^{-5}	2.097×10^{-5}	0.7154
90	0.9718	1008	0.03024	3.086×10^{-5}	2.139×10^{-5}	2.201×10^{-5}	0.7132
100	0.9458	1009	0.03095	3.243×10^{-5}	2.181×10^{-5}	2.306×10^{-5}	0.7111
120	0.8977	1011	0.03235	3.565×10^{-5}	2.264×10^{-5}	2.522×10^{-5}	0.7073
140	0.8542	1013	0.03374	3.898×10^{-5}	2.345×10^{-5}	2.745×10^{-5}	0.7041
160	0.8148	1016	0.03511	4.241×10^{-5}	2.420×10^{-5}	2.975×10^{-5}	0.7014
180	0.7788	1019	0.03646	4.593×10^{-5}	2.504×10^{-5}	3.212×10^{-5}	0.6992
200	0.7459	1023	0.03779	4.954×10^{-5}	2.577×10^{-5}	3.455×10^{-5}	0.6974
250	0.6746	1033	0.04104	5.890×10^{-5}	2.760×10^{-5}	4.091×10^{-5}	0.6946
300	0.6158	1044	0.04418	6.871×10^{-5}	2.934×10^{-5}	4.765×10^{-5}	0.6935
350	0.5664	1056	0.04721	7.892×10^{-5}	3.101×10^{-5}	5.475×10^{-5}	0.6937
400	0.5243	1069	0.05015	8.951×10^{-5}	3.261×10^{-5}	6.219×10^{-5}	0.6948
450	0.4880	1081	0.05298	1.004×10^{-4}	3.415×10^{-5}	6.997×10^{-5}	0.6965
500	0.4565	1093	0.05572	1.117×10^{-4}	3.563×10^{-5}	7.806×10^{-5}	0.6986
600	0.4042	1115	0.06093	1.352×10^{-4}	3.846×10^{-5}	9.515×10^{-5}	0.7037
700	0.3627	1135	0.06581	1.598×10^{-4}	4.111×10^{-5}	1.133×10^{-4}	0.7092
800	0.3289	1153	0.07037	1.855×10^{-4}	4.362×10^{-5}	1.326×10^{-4}	0.7149
900	0.3008	1169	0.07465	2.122×10^{-4}	4.600×10^{-5}	1.529×10^{-4}	0.7206
1000	0.2772	1184	0.07868	2.398×10^{-4}	4.826×10^{-5}	1.741×10^{-4}	0.7260
1500	0.1990	1234	0.09599	3.908×10^{-4}	5.817×10^{-5}	2.922×10^{-4}	0.7478
2000	0.1553	1264	0.11113	5.664×10^{-4}	6.630×10^{-5}	4.270×10^{-4}	0.7539

Figure 34 Properties of Air at 1 atm [2]

APPENDIX II: SIMULATION DATA

Airfoil Curve Points: X, Y

NACA 0012		0.65434	0.04093	0.21951	0.05836
1.00000	0.00126	0.62492	0.04354	0.19760	0.05723
0.99280	0.00227	0.59547	0.04600	0.17661	0.05581
0.97989	0.00405	0.56607	0.04832	0.15660	0.05410
0.96352	0.00627	0.53680	0.05047	0.13760	0.05211
0.94455	0.00878	0.50774	0.05245	0.11965	0.04983
0.92350	0.01151	0.47895	0.05422	0.10280	0.04729
0.90075	0.01438	0.45050	0.05578	0.08709	0.04450
0.87658	0.01735	0.42246	0.05712	0.07256	0.04145
0.85123	0.02038	0.39488	0.05822	0.05924	0.03817
0.82489	0.02343	0.36782	0.05906	0.04717	0.03467
0.79774	0.02648	0.34135	0.05965	0.03639	0.03096
0.76991	0.02950	0.31551	0.05996	0.02694	0.02705
0.74154	0.03248	0.29035	0.06000	0.01885	0.02296
0.71275	0.03539	0.26594	0.05974	0.01215	0.01869
0.68365	0.03821	0.24231	0.05920	0.00688	0.01425

0.00308	0.00965	0.19760	-0.05723	0.71275	-0.03539
0.00078	0.00490	0.21951	-0.05836	0.74154	-0.03248
0.00000	0.00000	0.24231	-0.05920	0.76991	-0.02950
0.00078	-0.00490	0.26594	-0.05974	0.79774	-0.02648
0.00308	-0.00965	0.29035	-0.06000	0.82489	-0.02343
0.00688	-0.01425	0.31551	-0.05996	0.85123	-0.02038
0.01215	-0.01869	0.34135	-0.05965	0.87658	-0.01735
0.01885	-0.02296	0.36782	-0.05906	0.90075	-0.01438
0.02694	-0.02705	0.39488	-0.05822	0.92350	-0.01151
0.03639	-0.03096	0.42246	-0.05712	0.94455	-0.00878
0.04717	-0.03467	0.45050	-0.05578	0.96352	-0.00627
0.05924	-0.03817	0.47895	-0.05422	0.97989	-0.00405
0.07256	-0.04145	0.50774	-0.05245	0.99280	-0.00227
0.08709	-0.04450	0.53680	-0.05047	1.00000	-0.00126
0.10280	-0.04729	0.56607	-0.04832		
0.11965	-0.04983	0.59547	-0.04600		
0.13760	-0.05211	0.62492	-0.04354		
0.15660	-0.05410	0.65434	-0.04093		
0.17661	-0.05581	0.68365	-0.03821		

NACA 0015		0.56607	0.06040	0.10280	0.05912
1.00000	0.00157	0.53680	0.06309	0.08709	0.05562
0.99280	0.00283	0.50774	0.06556	0.07256	0.05182
0.97989	0.00506	0.47895	0.06777	0.05924	0.04772
0.96352	0.00783	0.45050	0.06973	0.04717	0.04334
0.94455	0.01098	0.42246	0.07140	0.03639	0.03870
0.92350	0.01439	0.39488	0.07277	0.02694	0.03381
0.90075	0.01798	0.36782	0.07383	0.01885	0.02870
0.87658	0.02169	0.34135	0.07456	0.01215	0.02336
0.85123	0.02548	0.31551	0.07495	0.00688	0.01781
0.82489	0.02929	0.29035	0.07500	0.00308	0.01207
0.79774	0.03310	0.26594	0.07468	0.00078	0.00613
0.76991	0.03688	0.24231	0.07400	0.00000	0.00000
0.74154	0.04060	0.21951	0.07296	0.00078	-0.00613
0.71275	0.04423	0.19760	0.07154	0.00308	-0.01207
0.68365	0.04776	0.17661	0.06977	0.00688	-0.01781
0.65434	0.05117	0.15660	0.06763	0.01215	-0.02336
0.62492	0.05442	0.13760	0.06513	0.01885	-0.02870
0.59547	0.05751	0.11965	0.06229	0.02694	-0.03381

0.03639	-0.03870	0.42246	-0.07140	0.94455	-0.01098
0.04717	-0.04334	0.45050	-0.06973	0.96352	-0.00783
0.05924	-0.04772	0.47895	-0.06777	0.97989	-0.00506
0.07256	-0.05182	0.50774	-0.06556	0.99280	-0.00283
0.08709	-0.05562	0.53680	-0.06309	1.00000	-0.00157
0.10280	-0.05912	0.56607	-0.06040		
0.11965	-0.06229	0.59547	-0.05751		
0.13760	-0.06513	0.62492	-0.05442		
0.15660	-0.06763	0.65434	-0.05117		
0.17661	-0.06977	0.68365	-0.04776		
0.19760	-0.07154	0.71275	-0.04423		
0.21951	-0.07296	0.74154	-0.04060		
0.24231	-0.07400	0.76991	-0.03688		
0.26594	-0.07468	0.79774	-0.03310		
0.29035	-0.07500	0.82489	-0.02929		
0.31551	-0.07495	0.85123	-0.02548		
0.34135	-0.07456	0.87658	-0.02169		
0.36782	-0.07383	0.90075	-0.01798		
0.39488	-0.07277	0.92350	-0.01439		

NACA 0018		0.56607	0.07248	0.10280	0.07094
1.00000	0.00189	0.53680	0.07571	0.08709	0.06674
0.99280	0.00340	0.50774	0.07867	0.07256	0.06218
0.97989	0.00607	0.47895	0.08133	0.05924	0.05726
0.96352	0.00940	0.45050	0.08367	0.04717	0.05201
0.94455	0.01318	0.42246	0.08568	0.03639	0.04644
0.92350	0.01727	0.39488	0.08733	0.02694	0.04058
0.90075	0.02158	0.36782	0.08860	0.01885	0.03443
0.87658	0.02603	0.34135	0.08947	0.01215	0.02803
0.85123	0.03057	0.31551	0.08994	0.00688	0.02137
0.82489	0.03515	0.29035	0.09000	0.00308	0.01448
0.79774	0.03972	0.26594	0.08962	0.00078	0.00735
0.76991	0.04426	0.24231	0.08880	0.00000	0.00000
0.74154	0.04872	0.21951	0.08755	0.00078	-0.00735
0.71275	0.05308	0.19760	0.08585	0.00308	-0.01448
0.68365	0.05732	0.17661	0.08372	0.00688	-0.02137
0.65434	0.06140	0.15660	0.08115	0.01215	-0.02803
0.62492	0.06530	0.13760	0.07816	0.01885	-0.03443
0.59547	0.06901	0.11965	0.07475	0.02694	-0.04058

0.03639	-0.04644	0.42246	-0.08568	0.94455	-0.01318
0.04717	-0.05201	0.45050	-0.08367	0.96352	-0.00940
0.05924	-0.05726	0.47895	-0.08133	0.97989	-0.00607
0.07256	-0.06218	0.50774	-0.07867	0.99280	-0.00340
0.08709	-0.06674	0.53680	-0.07571	1.00000	-0.00189
0.10280	-0.07094	0.56607	-0.07248		
0.11965	-0.07475	0.59547	-0.06901		
0.13760	-0.07816	0.62492	-0.06530		
0.15660	-0.08115	0.65434	-0.06140		
0.17661	-0.08372	0.68365	-0.05732		
0.19760	-0.08585	0.71275	-0.05308		
0.21951	-0.08755	0.74154	-0.04872		
0.24231	-0.08880	0.76991	-0.04426		
0.26594	-0.08962	0.79774	-0.03972		
0.29035	-0.09000	0.82489	-0.03515		
0.31551	-0.08994	0.85123	-0.03057		
0.34135	-0.08947	0.87658	-0.02603		
0.36782	-0.08860	0.90075	-0.02158		
0.39488	-0.08733	0.92350	-0.01727		

NACA 0020		0.56607	0.08054	0.10280	0.07882
1.00000	0.00210	0.53680	0.08412	0.08709	0.07416
0.99280	0.00378	0.50774	0.08741	0.07256	0.06909
0.97989	0.00675	0.47895	0.09037	0.05924	0.06362
0.96352	0.01044	0.45050	0.09297	0.04717	0.05779
0.94455	0.01464	0.42246	0.09520	0.03639	0.05160
0.92350	0.01918	0.39488	0.09703	0.02694	0.04509
0.90075	0.02397	0.36782	0.09844	0.01885	0.03826
0.87658	0.02892	0.34135	0.09942	0.01215	0.03114
0.85123	0.03397	0.31551	0.09994	0.00688	0.02375
0.82489	0.03905	0.29035	0.09999	0.00308	0.01609
0.79774	0.04414	0.26594	0.09957	0.00078	0.00817
0.76991	0.04917	0.24231	0.09867	0.00000	0.00000
0.74154	0.05413	0.21951	0.09727	0.00078	-0.00817
0.71275	0.05898	0.19760	0.09539	0.00308	-0.01609
0.68365	0.06368	0.17661	0.09302	0.00688	-0.02375
0.65434	0.06822	0.15660	0.09017	0.01215	-0.03114
0.62492	0.07256	0.13760	0.08684	0.01885	-0.03826
0.59547	0.07667	0.11965	0.08306	0.02694	-0.04509

0.03639	-0.05160	0.42246	-0.09520	0.94455	-0.01464
0.04717	-0.05779	0.45050	-0.09297	0.96352	-0.01044
0.05924	-0.06362	0.47895	-0.09037	0.97989	-0.00675
0.07256	-0.06909	0.50774	-0.08741	0.99280	-0.00378
0.08709	-0.07416	0.53680	-0.08412	1.00000	-0.00210
0.10280	-0.07882	0.56607	-0.08054		
0.11965	-0.08306	0.59547	-0.07667		
0.13760	-0.08684	0.62492	-0.07256		
0.15660	-0.09017	0.65434	-0.06822		
0.17661	-0.09302	0.68365	-0.06368		
0.19760	-0.09539	0.71275	-0.05898		
0.21951	-0.09727	0.74154	-0.05413		
0.24231	-0.09867	0.76991	-0.04917		
0.26594	-0.09957	0.79774	-0.04414		
0.29035	-0.09999	0.82489	-0.03905		
0.31551	-0.09994	0.85123	-0.03397		
0.34135	-0.09942	0.87658	-0.02892		
0.36782	-0.09844	0.90075	-0.02397		
0.39488	-0.09703	0.92350	-0.01918		

NACA 0021		0.56607	0.08456	0.10280	0.08276
1.00000	0.00220	0.53680	0.08833	0.08709	0.07787
0.99280	0.00396	0.50774	0.09178	0.07256	0.07254
0.97989	0.00708	0.47895	0.09488	0.05924	0.06680
0.96352	0.01097	0.45050	0.09762	0.04717	0.06068
0.94455	0.01537	0.42246	0.09996	0.03639	0.05418
0.92350	0.02014	0.39488	0.10188	0.02694	0.04734
0.90075	0.02517	0.36782	0.10336	0.01885	0.04017
0.87658	0.03037	0.34135	0.10439	0.01215	0.03270
0.85123	0.03567	0.31551	0.10494	0.00688	0.02494
0.82489	0.04101	0.29035	0.10499	0.00308	0.01689
0.79774	0.04634	0.26594	0.10455	0.00078	0.00858
0.76991	0.05163	0.24231	0.10360	0.00000	0.00000
0.74154	0.05684	0.21951	0.10214	0.00078	-0.00858
0.71275	0.06193	0.19760	0.10016	0.00308	-0.01689
0.68365	0.06687	0.17661	0.09767	0.00688	-0.02494
0.65434	0.07163	0.15660	0.09468	0.01215	-0.03270
0.62492	0.07619	0.13760	0.09118	0.01885	-0.04017
0.59547	0.08051	0.11965	0.08721	0.02694	-0.04734

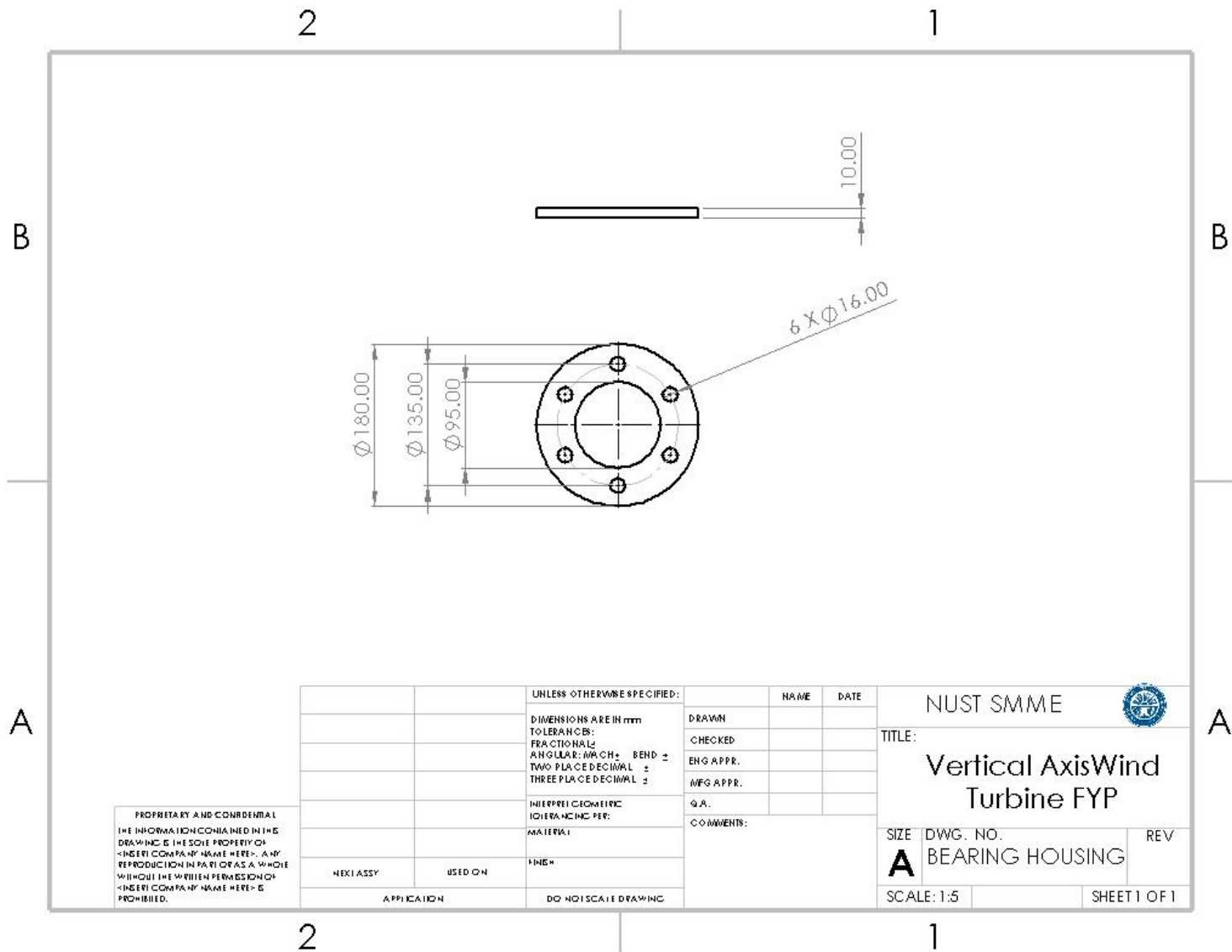
0.03639	-0.05418	0.42246	-0.09996	0.94455	-0.01537
0.04717	-0.06068	0.45050	-0.09762	0.96352	-0.01097
0.05924	-0.06680	0.47895	-0.09488	0.97989	-0.00708
0.07256	-0.07254	0.50774	-0.09178	0.99280	-0.00396
0.08709	-0.07787	0.53680	-0.08833	1.00000	-0.00220
0.10280	-0.08276	0.56607	-0.08456		
0.11965	-0.08721	0.59547	-0.08051		
0.13760	-0.09118	0.62492	-0.07619		
0.15660	-0.09468	0.65434	-0.07163		
0.17661	-0.09767	0.68365	-0.06687		
0.19760	-0.10016	0.71275	-0.06193		
0.21951	-0.10214	0.74154	-0.05684		
0.24231	-0.10360	0.76991	-0.05163		
0.26594	-0.10455	0.79774	-0.04634		
0.29035	-0.10499	0.82489	-0.04101		
0.31551	-0.10494	0.85123	-0.03567		
0.34135	-0.10439	0.87658	-0.03037		
0.36782	-0.10336	0.90075	-0.02517		
0.39488	-0.10188	0.92350	-0.02014		

NACA 2412		0.56607	0.06679	0.10280	0.05625
1.00000	0.00126	0.53680	0.06944	0.08709	0.05226
0.99280	0.00274	0.50774	0.07180	0.07256	0.04805
0.97989	0.00537	0.47895	0.07387	0.05924	0.04366
0.96352	0.00862	0.45050	0.07564	0.04717	0.03911
0.94455	0.01231	0.42246	0.07709	0.03639	0.03443
0.92350	0.01629	0.39488	0.07821	0.02694	0.02965
0.90075	0.02045	0.36782	0.07893	0.01885	0.02480
0.87658	0.02474	0.34135	0.07922	0.01215	0.01988
0.85123	0.02907	0.31551	0.07907	0.00688	0.01493
0.82489	0.03340	0.29035	0.07849	0.00308	0.00996
0.79774	0.03769	0.26594	0.07750	0.00078	0.00498
0.76991	0.04190	0.24231	0.07609	0.00000	0.00000
0.74154	0.04600	0.21951	0.07429	0.00078	-0.00482
0.71275	0.04995	0.19760	0.07211	0.00308	-0.00935
0.68365	0.05374	0.17661	0.06957	0.00688	-0.01357
0.65434	0.05734	0.15660	0.06670	0.01215	-0.01749
0.62492	0.06073	0.13760	0.06350	0.01885	-0.02112
0.59547	0.06388	0.11965	0.06001	0.02694	-0.02445

0.03639	-0.02749	0.42246	-0.03715	0.94455	-0.00526
0.04717	-0.03023	0.45050	-0.03592	0.96352	-0.00391
0.05924	-0.03269	0.47895	-0.03457	0.97989	-0.00273
0.07256	-0.03485	0.50774	-0.03309	0.99280	-0.00179
0.08709	-0.03674	0.53680	-0.03151	1.00000	-0.00126
0.10280	-0.03833	0.56607	-0.02985		
0.11965	-0.03966	0.59547	-0.02813		
0.13760	-0.04071	0.62492	-0.02635		
0.15660	-0.04151	0.65434	-0.02453		
0.17661	-0.04205	0.68365	-0.02268		
0.19760	-0.04236	0.71275	-0.02082		
0.21951	-0.04244	0.74154	-0.01896		
0.24231	-0.04231	0.76991	-0.01711		
0.26594	-0.04199	0.79774	-0.01527		
0.29035	-0.04150	0.82489	-0.01346		
0.31551	-0.04086	0.85123	-0.01169		
0.34135	-0.04008	0.87658	-0.00997		
0.36782	-0.03919	0.90075	-0.00831		
0.39488	-0.03822	0.92350	-0.00674		

Table 5 Solidworks Results

Goal Name	Unit	Value	Averaged Value	Minimum Value	Maximum Value	Progress [%]	Use In Convergence	Delta	Criteria
GG Average Total Pressure 1	[Pa]	101363.3637	101363.203	101362.9639	101363.4823	100	Yes	0.091118049	0.938900582
GG Average Velocity 2	[m/s]	7.48571833	7.54473571	7.48571833	7.567701737	5.9	Yes	0.0772194	0.004560289
GG Force (Z) 3	[N]	-19.4368889	-19.58071239	-19.80075939	-19.25773054	100	Yes	0.209445448	4.543856204
GG Torque (Y) 4	[N*m]	-31.1779664	-31.19061659	-31.24524229	-31.12116285	100	Yes	0.124079441	0.755961415
Inlet Pressure	[Pa]	101372.6973	101372.606	101372.4067	101373.0404	100	Yes	0.358920456	2.229446313
Inlet Velocity	[m/s]	8.072015526	8.067078211	8.051299159	8.082637979	64.8	Yes	0.03133882	0.020326999
Outlet Pressure	[Pa]	101328.6762	101327.1522	101325.9166	101328.6762	100	Yes	0.777801535	6.081318037
Outlet Velocity	[m/s]	1.970469864	2.019124182	1.969561219	2.132769623	83.5	Yes	0.163208404	0.136377087
SG Average Total Pressure 1	[Pa]	101735.7829	101734.9599	101734.5849	101735.7829	100	Yes	0.952814123	76.97418593
SG Average Velocity 2	[m/s]	26.64992033	26.64992033	26.64992033	26.64992033	100	Yes	0	2.66499E-07
SG Force (X) 3	[N]	-5.28181758	-5.051713526	-5.560153081	-4.630081299	100	Yes	0.133426118	59.24169619
SG Force (Y) 4	[N]	-0.02516328	-0.035489728	-0.045626938	-0.025163279	100	Yes	0.015199985	0.209978855
SG Force (Z) 5	[N]	-14.4976264	-15.14811042	-15.80501193	-14.48875093	100	Yes	1.128749994	29.05073002
SG Torque (Y) 6	[N*m]	-10.1390604	-10.06873345	-10.14616138	-9.983199478	100	Yes	0.162961898	5.483232579
Coefficient of Power	[]	0.40030468	0.400467098	0.401168456	0.399575358	100	Yes	0.001593099	0.00970605



PROPRIETARY AND CONFIDENTIAL
 THE INFORMATION CONTAINED IN THIS
 DRAWING IS THE SOLE PROPERTY OF
 <INSERT COMPANY NAME HERE>. ANY
 REPRODUCTION IN PART OR AS A WHOLE
 WITHOUT THE WRITTEN PERMISSION OF
 <INSERT COMPANY NAME HERE> IS
 PROHIBITED.

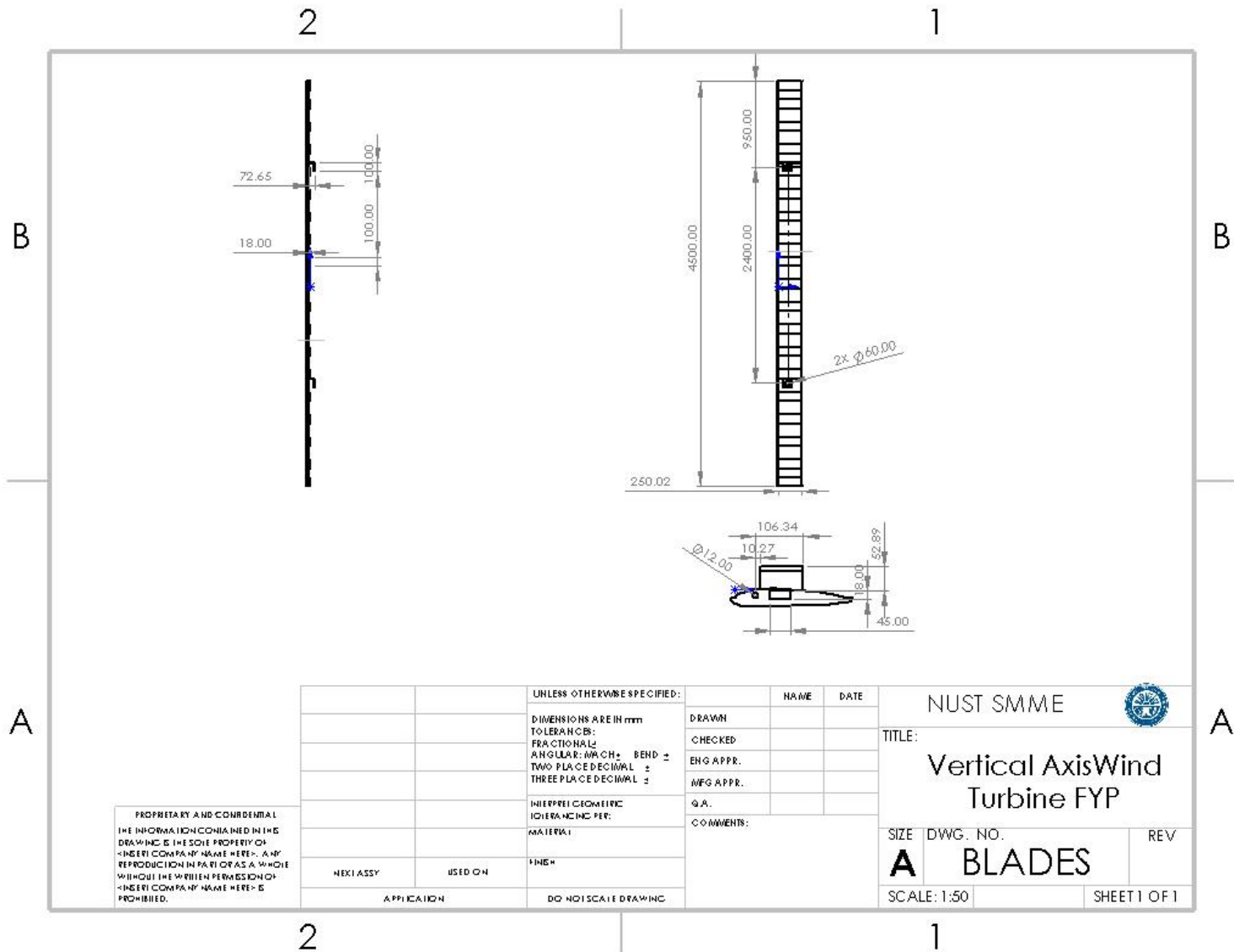
		UNLESS OTHERWISE SPECIFIED:	NAME	DATE
		DIMENSIONS ARE IN mm	DRAWN	
		TOLERANCES:	CHECKED	
		FRACTIONALS: ±	ENG APPR.	
		ANGULAR: MM CH. BEND ±	MFG APPR.	
		TWO PLACE DECIMAL ±	Q.A.	
		THREE PLACE DECIMAL ±	COMMENTS:	
		INTERPRET GEOMETRIC TOLERANCING PER:		
		MATERIAL:		
		FINE:		
NEXT ASSY	USED ON	APPLICATION		
		DO NOT SCALE DRAWING		

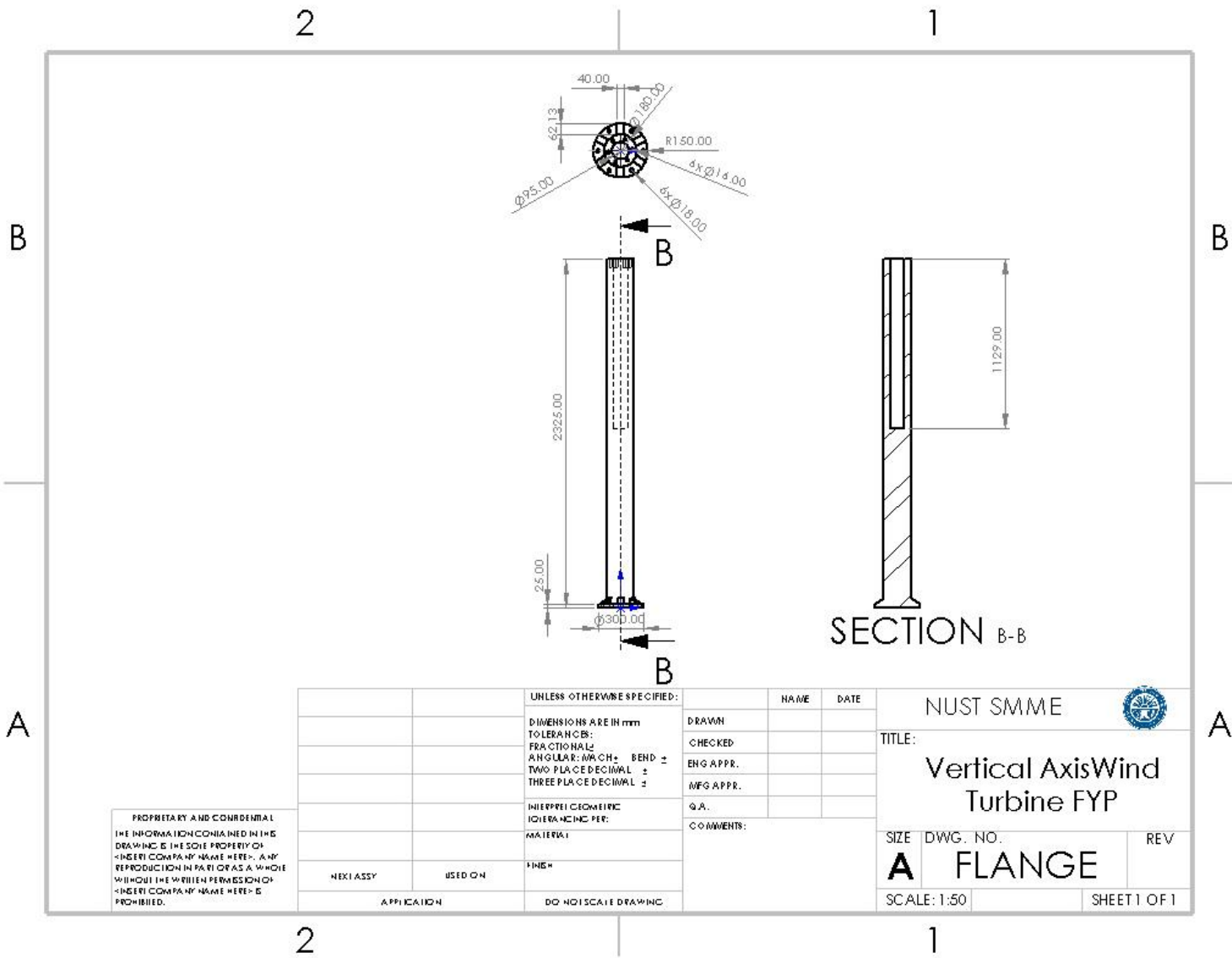
NUST SMME 

TITLE:
**Vertical Axis Wind
 Turbine FYP**

SIZE **A** DWG. NO. BEARING HOUSING REV

SCALE: 1:5 SHEET 1 OF 1





PROPRIETARY AND CONFIDENTIAL
 THE INFORMATION CONTAINED IN THIS
 DRAWING IS THE SOLE PROPERTY OF
 NUST COMPANY NAME HERE. ANY
 REPRODUCTION IN PART OR AS A WHOLE
 WITHOUT THE WRITTEN PERMISSION OF
 NUST COMPANY NAME HERE IS
 PROHIBITED.

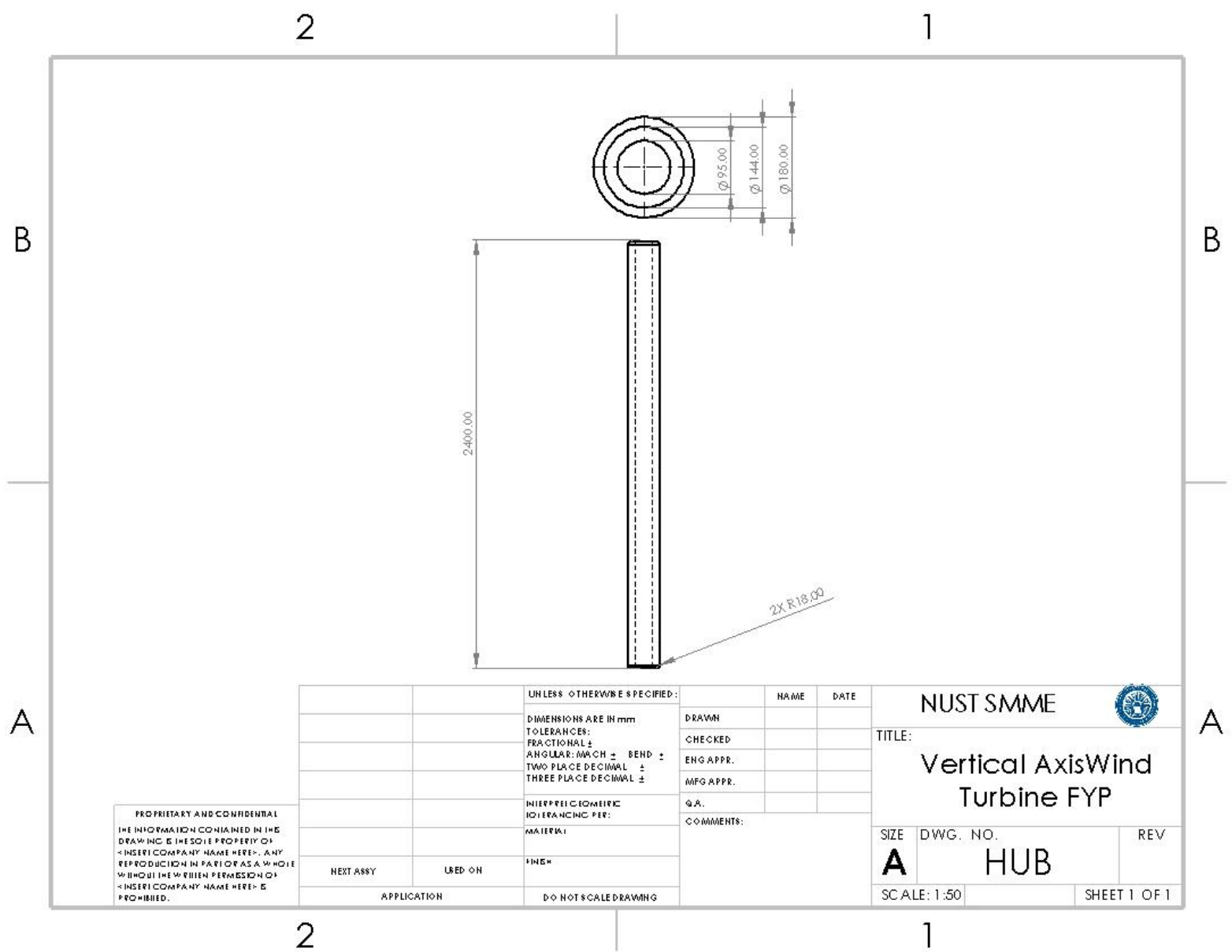
UNLESS OTHERWISE SPECIFIED:		NAME	DATE
DIMENSIONS ARE IN mm		DRAWN	
TOLERANCES:		CHECKED	
FRACTIONALS		ENG APPR.	
ANGULAR: MATCH BEND ±		MFG APPR.	
TWO PLACE DECIMAL ±		Q.A.	
THREE PLACE DECIMAL ±		COMMENTS:	
INTERPRET GEOMETRIC TOLERANCING PER:			
MATERIAL:			
FINISH:			
NEXT ASSY	USED ON		
APPLICATION			
DO NOT SCALE DRAWING			

NUST SMME 

TITLE:
**Vertical Axis Wind
 Turbine FYP**

SIZE DWG. NO. REV
A FLANGE

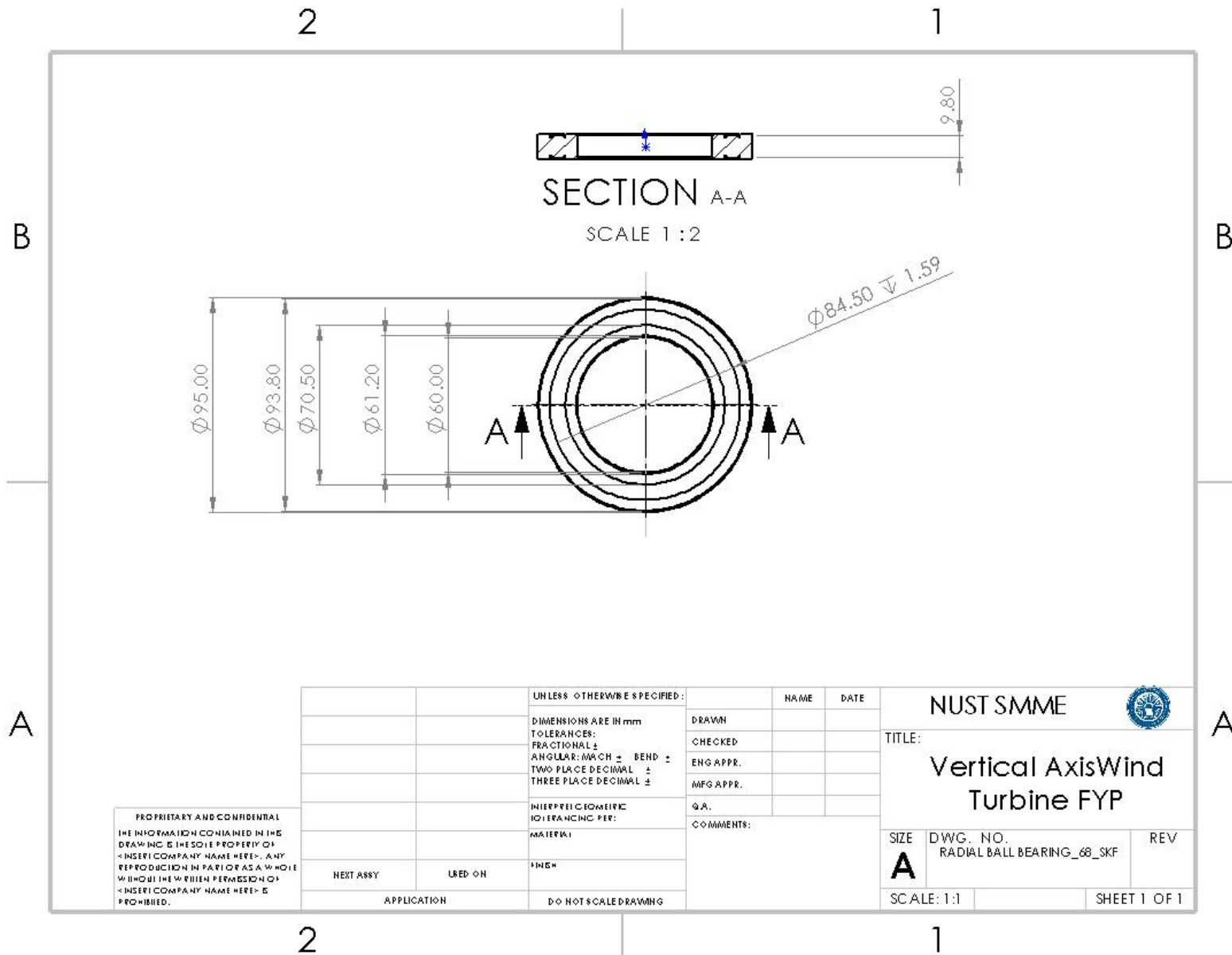
SCALE: 1:50 SHEET 1 OF 1



PROPRIETARY AND CONFIDENTIAL
 THE INFORMATION CONTAINED IN THIS
 DRAWING IS THE SOLE PROPERTY OF
 <INSERT COMPANY NAME HERE>. ANY
 REPRODUCTION IN PART OR AS A WHOLE
 WITHOUT THE WRITTEN PERMISSION OF
 <INSERT COMPANY NAME HERE> IS
 PROHIBITED.

		UNLESS OTHERWISE SPECIFIED:		NAME	DATE
		DIMENSIONS ARE IN mm	DRAWN		
		TOLERANCES:	CHECKED		
		FRACTIONAL ±	ENG APPR.		
		ANGULAR: MATCH ± BEND ±	MFG APPR.		
		TWO PLACE DECIMAL ±	Q.A.		
		THREE PLACE DECIMAL ±	COMMENTS:		
		MATERIAL:			
		FINISH:			
NEXT ASSY	USED ON				
APPLICATION		DO NOT SCALE DRAWING			

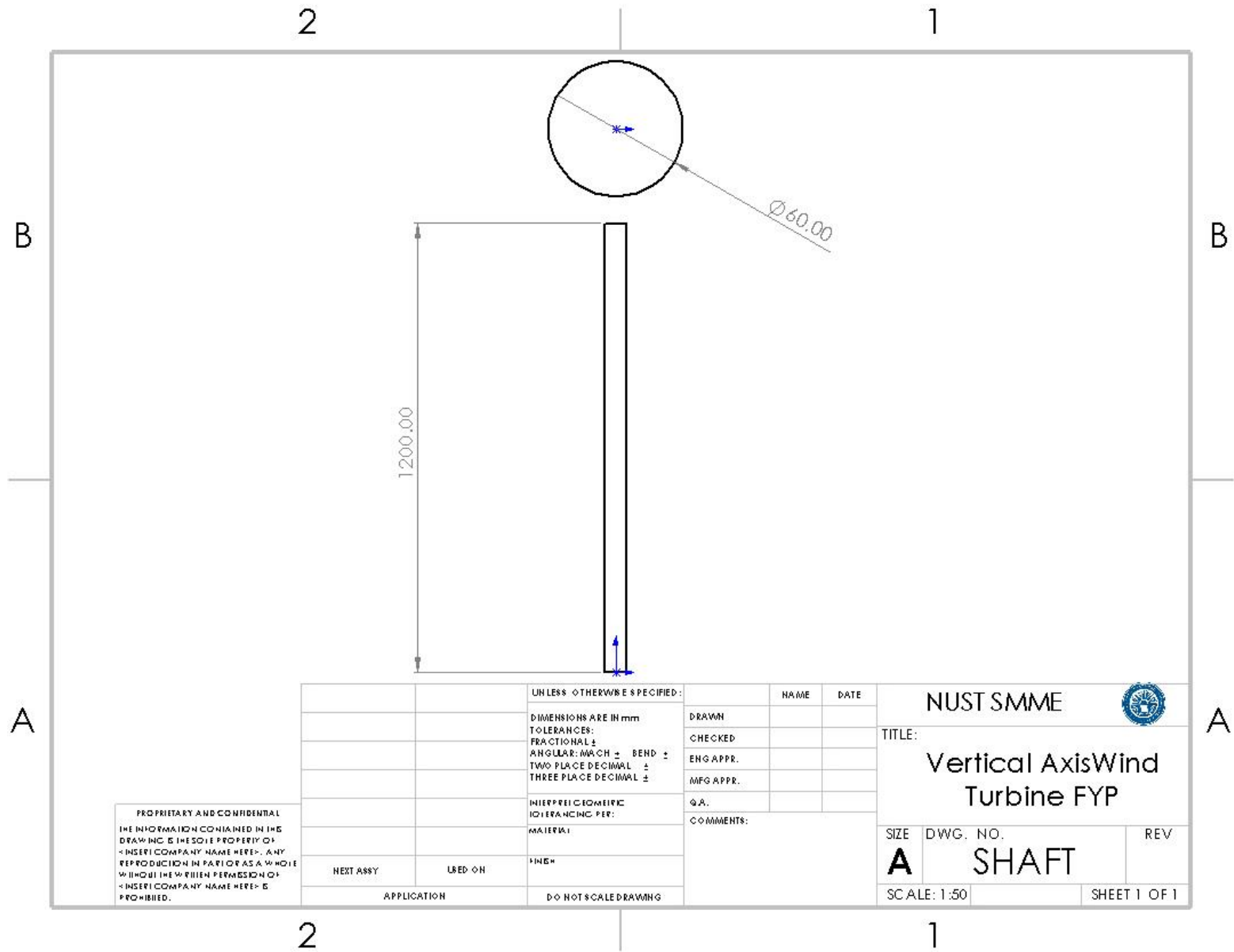
MUST SMME 
 TITLE:
**Vertical Axis Wind
 Turbine FYP**
 SIZE: **A** DWG. NO. **HUB** REV
 SCALE: 1:50 SHEET 1 OF 1



PROPRIETARY AND CONFIDENTIAL
 THE INFORMATION CONTAINED IN THIS
 DRAWING IS THE SOLE PROPERTY OF
 <INSERT COMPANY NAME HERE>. ANY
 REPRODUCTION IN PART OR AS A WHOLE
 WITHOUT THE WRITTEN PERMISSION OF
 <INSERT COMPANY NAME HERE> IS
 PROHIBITED.

		UNLESS OTHERWISE SPECIFIED:		NAME	DATE
		DIMENSIONS ARE IN mm	DRAWN		
		TOLERANCES:	CHECKED		
		FRACTIONAL ±	ENG APPR.		
		ANGULAR: MAJOR ± BEND ±	MFG APPR.		
		TWO PLACE DECIMAL ±	Q.A.		
		THREE PLACE DECIMAL ±	COMMENTS:		
		INTERFERENCE FITS:			
		MATERIAL:			
		FINISH:			
NEXT ASSY	USED ON				
APPLICATION		DO NOT SCALE DRAWING			

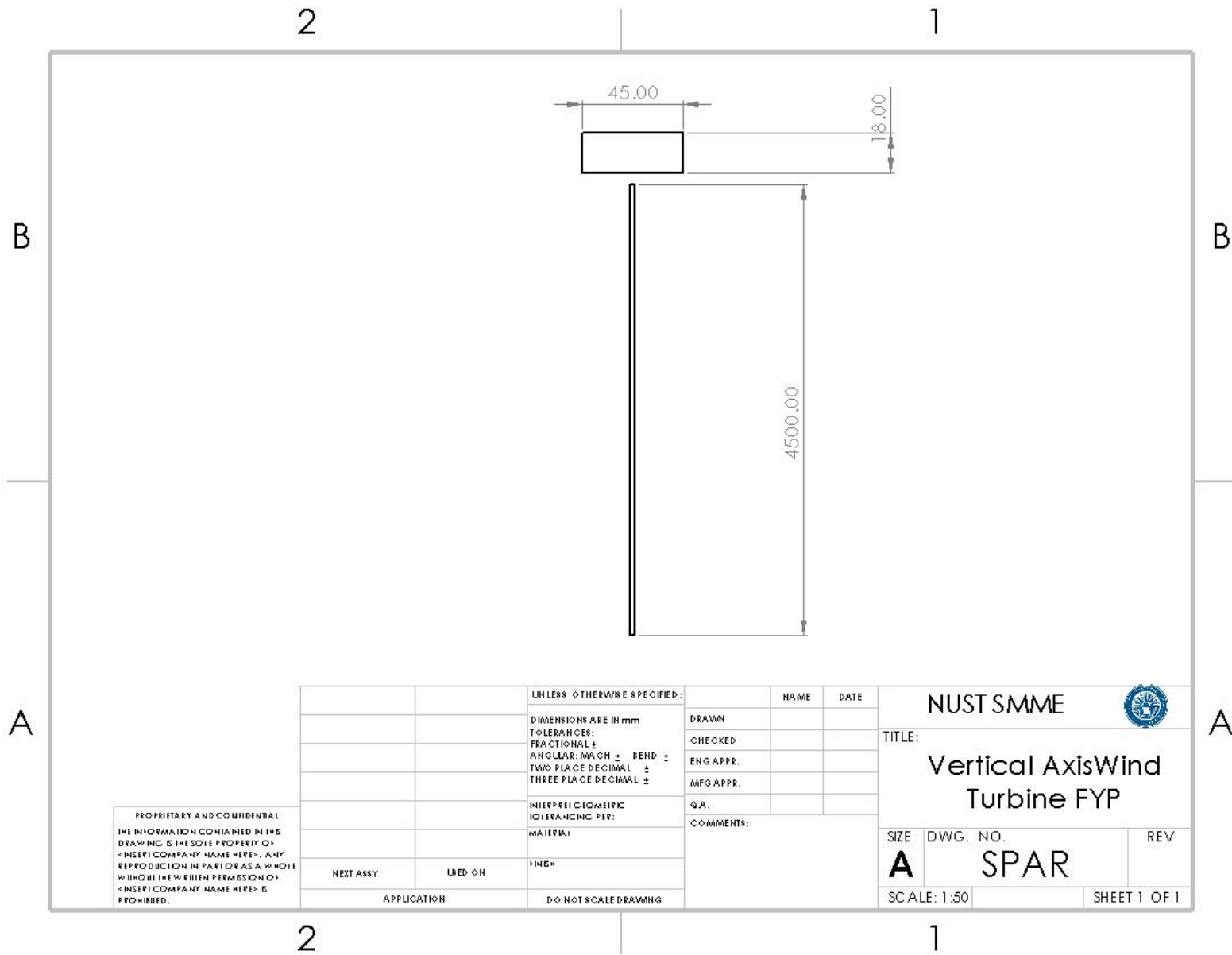
NUST SMME		
TITLE:		
Vertical Axis Wind Turbine FYP		
SIZE	DWG. NO.	REV
A	RADIAL BALL BEARING_68 SKF	
SCALE: 1:1	SHEET 1 OF 1	



PROPRIETARY AND CONFIDENTIAL
 THE INFORMATION CONTAINED IN THE
 DRAWING IS THE SOLE PROPERTY OF
 ~ INSERT COMPANY NAME HERE ~. ANY
 REPRODUCTION IN PART OR AS A WHOLE
 WITHOUT THE WRITTEN PERMISSION OF
 ~ INSERT COMPANY NAME HERE ~ IS
 PROHIBITED.

UNLESS OTHERWISE SPECIFIED:		NAME	DATE
DIMENSIONS ARE IN mm		DRAWN	
TOLERANCES:		CHECKED	
FRACTIONAL ±		ENG APPR.	
ANGULAR: MACH ± BEND ±		MFG APPR.	
TWO PLACE DECIMAL ±		Q.A.	
THREE PLACE DECIMAL ±		COMMENTS:	
INTERPRETATION/PER:			
MATERIAL:			
FINISH:			
NEXT ASSY	USED ON		
APPLICATION	DO NOT SCALE DRAWING		

NUST SMME 		
TITLE: Vertical Axis Wind Turbine FYP		
SIZE A	DWG. NO. SHAFT	REV
SCALE: 1:50	SHEET 1 OF 1	



PROPRIETARY AND CONFIDENTIAL
 THE INFORMATION CONTAINED IN THIS
 DRAWING IS THE SOLE PROPERTY OF
 <INSERT COMPANY NAME HERE>. ANY
 REPRODUCTION IN PART OR AS A WHOLE
 WITHOUT THE WRITTEN PERMISSION OF
 <INSERT COMPANY NAME HERE> IS
 PROHIBITED.

UNLESS OTHERWISE SPECIFIED:		NAME	DATE
DIMENSIONS ARE IN mm		DRAWN	
TOLERANCES:		CHECKED	
FRACTIONAL ±		ENG APPR.	
ANGULAR: MACH ± BEND ±		MFG APPR.	
TWO PLACE DECIMAL ±		Q.A.	
THREE PLACE DECIMAL ±		COMMENTS:	
HIERARCHIC TOLERANCING PER:			
MATERIAL:			
FINISH:			
NEXT ASSY	USED ON		
APPLICATION		DO NOT SCALE DRAWING	

MUST SMME 		
TITLE:		
Vertical Axis Wind Turbine FYP		
SIZE	DWG. NO.	REV
A	SPAR	
SCALE: 1:50		SHEET 1 OF 1